

國立交通大學

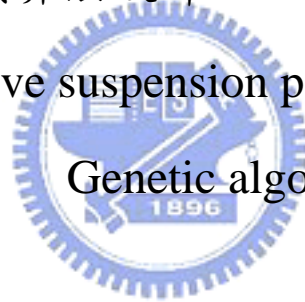
機械工程學系

碩士論文

利用基因演算法設計 ATV 之被動式懸吊參數

Design of passive suspension parameters for ATV using

Genetic algorithm



研究生：徐偉鈞

指導教授：成維華 教授

中華民國九十六年六月

利用基因演算法設計 ATV 之被動式懸吊參數

Design of passive suspension parameters for ATV using Genetic
algorithm

研究生：徐偉鈞

Student : Wei-Chun Hsu

指導教授：成維華

Advisor : Wei-Hua Chieng



A Thesis

Submitted to Institute of Mechanical Engineering

College of Engineering

National Chiao Tung University

in partial Fulfillment of the Requirements

for the Degree of

Master

In

Mechanical Engineering

June 2007

Hsinchu, Taiwan, Republic of China

中華民國九十六年六月


利用基因演算法設計 ATV 之被動式懸吊參數

研究生:徐偉鈞

指導教授:成維華 教授

國立交通大學機械工程學系研究所

摘 要



第一輛 ATV(all-terrain vehicle)在 1950 年被製造出來後，發展至今分為運動以及多用途兩大類。在戶外休閒風潮的帶動之下，運動型 ATV 的各方面性能也受到更多重視。其中為了增進操控性以及駕駛人員的舒適性，懸吊系統的設計尤為重要。被動式懸吊系統被廣泛用於 ATV 上，相較於主動式以及半主動式懸吊，被動式懸吊有構造相對簡單以及價格較為便宜的優點。本文主旨為利用全域最佳化的方法，配合事先取得不同行駛路面之資訊，求得最適的被動式懸吊參數設定，以求改進路面顛簸所傳至人體所產生的不舒適感。模擬結果顯示利用基因演算法之全域最佳化方法，能夠順利求的對特定行駛路面之最佳懸吊參數設定，並能有效的減緩駕駛人之不舒適感。


Design of passive suspension parameters for ATV using Genetic algorithm

Student : Wei-Chun Hsu

Advisor : Dr. Wei-Hua Chieng

Institute of Mechanical Engineering
National Chiao Tung University

Abstract

The logo of National Chiao Tung University is a circular emblem with a gear-like border. Inside the circle, there are stylized letters 'NCTU' and the year '1896' at the bottom.

The first ATVs (all-terrain vehicle) were made during 1950s. After 4-wheels models were developed, models continue today to be divided into the sport and utility markets. Following the raising of tendency toward outdoor recreation, the performance of sport ATVs was emphasized. The main objectives of vehicle suspension system are improving vehicle handling and improve comfort for passenger. Generally passive suspension systems were used on ATVs. Passive suspension systems are less expensive and easier to maintain. The objective of this paper is using global optimization method and pre-obtained road profiles to find the appropriate suspension parameters setting and improve the comfort of ATV drivers. The results show that genetic algorithm can find the optimal setting of suspension parameters and effectively reduce the discomfort of ATV drivers.

誌謝

首先誠摯的感謝指導教授成維華博士，兩年來老師的悉心指導，並不時的討論與指點我正確的方向，使我在這段求學的時間獲益良多。老師對學問的嚴謹態度更是我們學習的典範。

兩年的日子說長不長，說短還真短，一眨眼就過了。這段時間在實驗室共同生活的點滴，研究方面的討論、熬夜趕討人厭的作業、面對每個禮拜即將到來的meeting的恐懼、言不及義的閒聊、在這樣的無限迴圈中過完了可能是人生中最後一段求學的日子，感謝實驗室的學長學弟以及同學們，這段回憶因為有你們而令人難忘。

感謝Jack、黑人、葛雷學長在我遇到研究的困難時，總能適時的伸出援手，討論並指引我方向，給我莫大的助益，尤其感謝黑人常載我們去吃宵；感謝侯兄、明欣、建成兄、曹兄，雖然你們對本論文沒有實質的幫助，但給了我平日不可或缺的精神上的支持，恭喜我們一起順利捱過這兩年；感謝磊哥，星雲大師、強哥、文彬、洋豪、小賴，因為有了你們，實驗室總能充滿歡樂。交大的時間雖然不長，課業的壓力卻總是讓人覺得度日如年，尤其是在口試前夕，但是因為有了你們的陪伴，讓苦悶的研究所生活也變的多彩多姿。

最後，謹以此文獻給在求學的路上無條件支持我的父母。

Contents

摘要.....	i
Abstract	ii
誌謝.....	iii
Contents	iv
List of Figures	vi
List of tables	viii
Chapter 1 Introduction	1
1.1 Development of ATVs.....	1
1.2 Literature review.....	2
1.3 Motives and objectives.....	4
Chapter 2 Dynamic model of ATV with suspension system	5
2.1 Derivations of equations of motion.....	5
2.2 Whole body vibration.....	11
2.3 Legislation.....	12
Chapter 3 Suspension optimization	16
3.1 History of Genetic Algorithm.....	16
3.2 GA procedures.....	17
3.3 Optimization of passive suspension.....	21
Chapter 4 Simulation results	23
4.1 Road profile data	23
4.2 Optimization results.....	24
4.3 Discussion.....	26
Chapter 5 Conclusion	28
Reference	30

Figures	32
Tables	49



List of Figures

Figure 1.1 Honda TRX250EX Sport ATV.....	32
Figure 1.2 Passive suspension systems.....	32
Figure 2.1 Full-car model of ATV.....	33
Figure 2.2 simulink model of ATV.....	33
Figure 2.3 Frequency weighting curves	34
Figure 2.4 Axes and weighting curves.....	34
Figure 2.5 Approximate weighting curve of W_k	35
Figure 2.6 Approximate weighting curve of W_d	35
Figure 3.1 gradient-based optimization algorithms.....	36
Figure 3.2 GA-based optimization algorithms.....	36
Figure 3.3 the scheme of procedure of GA	37
Figure 3.4 the penalty function of rattle space of suspension.....	37
Figure 3.5 illustration of crossover procedure.....	38
Figure 3.6 scheme of optimization for passive suspension.....	38
Figure 4.1 road profile one input from A and B.....	39
Figure 4.2 road profile one input from C and D.....	39
Figure 4.3 road profile one input from A and B.....	40
Figure 4.4 road profile one input from C and D.....	40
Figure 4.5 optimized weighted vertical acceleration \ddot{z} for road profile one.....	41
Figure 4.6 optimized weighted vertical acceleration \ddot{z} for road profile one between 6.8 and 8 sec.....	41
Figure 4.7 optimized weighted roll velocity $\dot{\alpha}$ for road profile one.....	42
Figure 4.8 optimized weighted roll velocity $\dot{\alpha}$ for road profile one	

between 6 and 8 sec.....	42
Figure 4.9 optimized weighted pitch velocity $\dot{\beta}$ for road profile one...	43
Figure 4.10 optimized weighted roll velocity $\dot{\beta}$ for road profile one between 6 and 8 sec.....	43
Figure 4.11 fitness of optimization for road profile one.....	44
Figure 4.12 optimized weighted vertical acceleration \ddot{z} for road profile two.....	45
Figure 4.13 optimized weighted vertical acceleration \ddot{z} for road profile two between 1.8 and 3.5 sec.....	45
Figure 4.14 optimized weighted roll velocity $\dot{\alpha}$ for road profile two...	46
Figure 4.15 optimized weighted roll velocity $\dot{\alpha}$ for road profile two between 1.5 and 4 sec.....	46
Figure 4.16 optimized weighted pitch velocity $\dot{\beta}$ for road profile two...	47
Figure 4.17 optimized weighted roll velocity $\dot{\beta}$ for road profile two between 1.5 and 3.5 sec.....	47
Figure 4.18 fitness of optimization for road profile two.....	48

List of Tables

Table 4.1 specification of Honda TRX250EX Sport ATV.....	49
Table 4.2 settings of genetic algorithm.....	49
Table 4.3 optimization results of road profile one.....	50
Table 4.4 optimization results of road profile two.....	50



Chapter 1 Introduction

1.1 Development of ATVs

The term "all-terrain vehicle" is used in a general sense to describe any of a number of small open motorized buggies and tricycles designed for off-road use. The American National Standards Institute (ANSI) defines an ATV as a vehicle that travels on low pressure tires, with a seat that is straddled by the operator, and with handlebars for steering control. Honda made the first three-wheeled ATV in 1970. The front end of 3-wheelers obviously has a single wheel making it lighter, and flipping backwards is a potential hazard, especially when climbing hills, so all manufacturers switch to 4-wheeled models in the late '80s.

Models continue today to be divided into the sport type and utility market. Figure 1.1 illustrated a sport ATV made by Honda. Sport models are built with performance, rather than utility. Sport models are generally small, light, two wheel drive vehicles which accelerate quickly, have a manual transmission, and run at speeds up to 90 miles per hour. To be successful at fast trail riding, an ATV must have light weight, high power, good suspension and a low center of gravity. Following the raising of outdoor recreation, the performance of sort type ATV is more emphasized.

Sport type ATVs were used on kinds of terrains, such as desert racing, hill climbing, ice racing etc. The vibration due to the rough road condition makes the passenger feel uncomfortable and a well adjusted suspension system will improve the car handling and more comfortable for passenger.

1.2 Literature review

Passive suspension system is widely used on ATVs. Compared with active suspension and semi-active suspension, passive suspension is cheaper and easier to adjust and repair. One degree-of-freedom or two degree-of-freedom quarter-car models are commonly employed in many areas of the automotive industry, including optimization of suspensions of vehicles [1]. A design optimization of quarter-car models with passive suspensions under random road excitation was proposed [2]. In that paper, evaluation of the vehicle performance is based on examination of three response quantities, that is, the maximum absolute acceleration of the passengers, the distance between the wheel subsystem and the car body and the force developed between the wheel and the ground.

Some evaluations of the vehicle comfort are also used to optimize vehicle suspension. A typical measure of comfort has the form shown in equation 1-1[3].

$$J = \int_0^t \ddot{z}(t)^2 dt \quad (1-1)$$

Car-body travel distance and velocity, as in equations 1-2 and 1-3 below, are also used [4].

$$J = \int_0^t z(t)^2 dt \quad (1-2)$$

$$J = \int_0^t \dot{z}(t) dt \quad (1-3)$$

The jerk (rate of change of acceleration) can also be used as a measure of comfort, use equation 1-4 [5]

$$J = \int_0^t \ddot{\ddot{z}}(t)^2 dt \quad (1-4)$$

Besides, the official European measure of comfort, Vibration Does Value, use fourth-order powers shown in equation 1-5 [6].

$$VDV = \left[\frac{T_s}{N} \sum_{n=1}^N a_w^4 \right]^{1/4} \quad (1-5)$$

In [7], equation 1-4 was used as the measure of comfort and evolutionary algorithm was applied to the optimization of the system parameters. An optimal design for passive suspension of a light rail vehicle also using evolutionary algorithm has been issued [8]. A systematic and effective optimization scheme for the design of vehicle passive suspension system was proposed [9] [10].

In this paper, equation 1-5 is chosen as one of the measures of comfort because it's more sensitive of acceleration and a full-car model is used to provide a three degree-of-freedom model of ATVs. The global optimization algorithm, Genetic algorithm (or evolutionary algorithm), is selected to optimize the passive suspension parameters.

1.3 Motives and objectives

ATVs are usually driven on rough terrains. In order to maintain the stability and improve the driving comfort, an effective method for designing suspension parameters is needed. A frame of optimization design was developed in this paper.

For passive suspension systems shown in Figure 1.2, the parameter such as spring coefficient k and damping coefficient c are untunable during driving. So the presetting of k and c affects the driving comfort significantly. Based on optimization algorithm, the optimized k and c

are designed suitable for certain terrain. Therefore, different terrains have corresponding different settings of k and c to improve driving comfort. Besides, the rattle-space limit is also concerned in this paper to insure the travel of suspension is within its safety limit.



Chapter 2 Dynamic model of ATV with passive suspension system

2.1 Derivations of equations of motion

The model we consider here has three degree-of-freedom including vertical displacement of the center of gravity, roll and pitch angles. A full-car model of ATV is illustrated in Figure 2.1. A and D are the front two passive suspensions, C and D are the rear two passive suspensions, and O is the center of gravity. \bar{Z}_A , \bar{Z}_B , \bar{Z}_C , \bar{Z}_D are the road profile inputs to the four suspensions, respectively. \bar{Z} is the vertical displacement along the z-axis. When vehicle rotated in the inertial reference, the included angles are roll, pitch, and yaw angles, with notations α , β , and γ respectively, called the Euler angles. The signs of rotate angles are according to right-hand rule. Here we assume γ is very small and can be neglected when driving alone a straight lane. Therefore, the rotation matrix of the vehicle can be represented as follow

$$R_v(\theta_x, \theta_y, \theta_z) = R_v(\theta_x, \theta_y) = (R_x, R_y)^{-1} = \begin{bmatrix} \cos \beta & \sin \alpha \sin \beta & \cos \alpha \sin \beta \\ 0 & \cos \alpha & -\sin \alpha \\ -\sin \beta & \sin \alpha \cos \beta & \cos \alpha \cos \beta \end{bmatrix} \quad (2-1)$$

where R_x and R_y are

$$\text{roll axis: } R_x(\alpha) = \begin{bmatrix} 1 & 0 & 0 \\ 0 & \cos \alpha & \sin \alpha \\ 0 & -\sin \alpha & \cos \alpha \end{bmatrix}$$

$$\text{pitch axis: } R_y(\beta) = \begin{bmatrix} \cos \beta & 0 & -\sin \beta \\ 0 & 1 & 0 \\ \sin \beta & 0 & \cos \alpha \end{bmatrix} \quad (2-2)$$

With the rotation matrix R_y , the rotated vectors from O to each suspension can be represented as follows

$$\begin{aligned} \overline{OA}' &= R_y(\theta_x, \theta_y) \cdot \overline{OA} + (\bar{Z} - \bar{Z}_0) = \begin{bmatrix} \frac{\ell}{2} \cos \beta + \frac{w}{2} \sin \alpha \sin \beta \\ \frac{w}{2} \cos \alpha \\ -\frac{\ell}{2} \sin \beta + \frac{w}{2} \sin \alpha \cos \beta \end{bmatrix} + (\bar{Z} - \bar{Z}_0) \\ \overline{OB}' &= R_y(\theta_x, \theta_y) \cdot \overline{OB} + (\bar{Z} - \bar{Z}_0) = \begin{bmatrix} -\frac{\ell}{2} \cos \beta + \frac{w}{2} \sin \alpha \sin \beta \\ \frac{w}{2} \cos \alpha \\ \frac{\ell}{2} \sin \beta + \frac{w}{2} \sin \alpha \cos \beta \end{bmatrix} + (\bar{Z} - \bar{Z}_0) \\ \overline{OC}' &= R_y(\theta_x, \theta_y) \cdot \overline{OC} + (\bar{Z} - \bar{Z}_0) = \begin{bmatrix} \frac{\ell}{2} \cos \beta - \frac{w}{2} \sin \alpha \sin \beta \\ -\frac{w}{2} \cos \alpha \\ \frac{\ell}{2} \sin \beta - \frac{w}{2} \sin \alpha \cos \beta \end{bmatrix} + (\bar{Z} - \bar{Z}_0) \\ \overline{OD}' &= R_y(\theta_x, \theta_y) \cdot \overline{OD} + (\bar{Z} - \bar{Z}_0) = \begin{bmatrix} \frac{\ell}{2} \cos \beta - \frac{w}{2} \sin \alpha \sin \beta \\ -\frac{w}{2} \cos \alpha \\ -\frac{\ell}{2} \sin \beta - \frac{w}{2} \sin \alpha \cos \beta \end{bmatrix} + (\bar{Z} - \bar{Z}_0) \quad (2-3) \end{aligned}$$

Here \bar{Z}_0 is the origin point of local reference. Then we can derive the vertical displacement of each suspension, and for simplicity, we applied linearization by assuming α and β were small.

$$\begin{aligned}
\bar{d}_A = \overline{OA}' - \overline{OA} &= \begin{bmatrix} \frac{\ell}{2}(\cos \beta - 1) + \frac{w}{2} \sin \alpha \sin \beta \\ \frac{w}{2}(\cos \alpha - 1) \\ -\frac{\ell}{2} \sin \beta + \frac{w}{2} \sin \alpha \cos \beta \end{bmatrix} + (\bar{Z} - \bar{Z}_0) \approx \left(-\frac{\ell}{2} \beta + \frac{w}{2} \alpha + z\right) \begin{bmatrix} 0 \\ 0 \\ 1 \end{bmatrix} \\
\bar{d}_B = \overline{OB}' - \overline{OB} &= \begin{bmatrix} -\frac{\ell}{2}(\cos \beta - 1) + \frac{w}{2} \sin \alpha \sin \beta \\ \frac{w}{2}(\cos \alpha - 1) \\ \frac{\ell}{2} \sin \beta + \frac{w}{2} \sin \alpha \cos \beta \end{bmatrix} + (\bar{Z} - \bar{Z}_0) \approx \left(\frac{\ell}{2} \beta + \frac{w}{2} \alpha + z\right) \begin{bmatrix} 0 \\ 0 \\ 1 \end{bmatrix} \\
\bar{d}_C = \overline{OC}' - \overline{OC} &= \begin{bmatrix} -\frac{\ell}{2}(\cos \beta - 1) - \frac{w}{2} \sin \alpha \sin \beta \\ -\frac{w}{2}(\cos \alpha - 1) \\ \frac{\ell}{2} \sin \beta - \frac{w}{2} \sin \alpha \cos \beta \end{bmatrix} + (\bar{Z} - \bar{Z}_0) \approx \left(\frac{\ell}{2} \beta - \frac{w}{2} \alpha + z\right) \begin{bmatrix} 0 \\ 0 \\ 1 \end{bmatrix} \\
\bar{d}_D = \overline{OD}' - \overline{OD} &= \begin{bmatrix} \frac{\ell}{2}(\cos \beta - 1) - \frac{w}{2} \sin \alpha \sin \beta \\ -\frac{w}{2}(\cos \alpha - 1) \\ -\frac{\ell}{2} \sin \beta - \frac{w}{2} \sin \alpha \cos \beta \end{bmatrix} + (\bar{Z} - \bar{Z}_0) \approx \left(-\frac{\ell}{2} \beta - \frac{w}{2} \alpha + z\right) \begin{bmatrix} 0 \\ 0 \\ 1 \end{bmatrix}
\end{aligned} \tag{2-4}$$

where we assume

$$\bar{Z}_0 = \begin{bmatrix} 0 \\ 0 \\ 0 \end{bmatrix} \tag{2-5}$$

To get the net vertical displacement of each suspension, we subtract the road input from vertical displacement of each suspension.

$$\bar{d}_A - \bar{z}_A = \left(-\frac{\ell}{2} \beta + \frac{w}{2} \alpha + z - z_A\right) \begin{bmatrix} 0 \\ 0 \\ 1 \end{bmatrix}, \dot{\bar{d}}_A - \dot{z}_A = \left(-\frac{\ell}{2} \dot{\beta} + \frac{w}{2} \dot{\alpha} + \dot{z} - \dot{z}_A\right) \begin{bmatrix} 0 \\ 0 \\ 1 \end{bmatrix}$$

$$\begin{aligned}
\bar{d}_B - \bar{z}_B &= \left(\frac{\ell}{2} \beta + \frac{w}{2} \alpha + z - z_B \right) \begin{bmatrix} 0 \\ 0 \\ 1 \end{bmatrix}, \dot{\bar{d}}_B - \dot{\bar{z}}_B = \left(\frac{\ell}{2} \dot{\beta} + \frac{w}{2} \dot{\alpha} + \dot{z} - \dot{z}_B \right) \begin{bmatrix} 0 \\ 0 \\ 1 \end{bmatrix} \\
\bar{d}_C - \bar{z}_C &= \left(\frac{\ell}{2} \beta - \frac{w}{2} \alpha + z - z_C \right) \begin{bmatrix} 0 \\ 0 \\ 1 \end{bmatrix}, \dot{\bar{d}}_C - \dot{\bar{z}}_C = \left(\frac{\ell}{2} \dot{\beta} - \frac{w}{2} \dot{\alpha} + \dot{z} - \dot{z}_C \right) \begin{bmatrix} 0 \\ 0 \\ 1 \end{bmatrix} \\
\bar{d}_D - \bar{z}_D &= \left(-\frac{\ell}{2} \beta - \frac{w}{2} \alpha + z - z_D \right) \begin{bmatrix} 0 \\ 0 \\ 1 \end{bmatrix}, \dot{\bar{d}}_D - \dot{\bar{z}}_D = \left(-\frac{\ell}{2} \dot{\beta} - \frac{w}{2} \dot{\alpha} + \dot{z} - \dot{z}_D \right) \begin{bmatrix} 0 \\ 0 \\ 1 \end{bmatrix}
\end{aligned} \tag{2-6}$$

With the net vertical displacement of each suspension and its first derivative, we can derive the equations of motion by applying Lagrangian Dynamics.

$$\begin{aligned}
T &= \frac{1}{2} m \dot{Z}^2 + \frac{1}{2} I_x \dot{\theta}_x^2 + \frac{1}{2} I_y \dot{\theta}_y^2 \\
V &= mg(\bar{Z} - \bar{Z}_0) + \frac{1}{2} k_A (\bar{d}_A - \bar{z}_A)^2 + \frac{1}{2} k_B (\bar{d}_B - \bar{z}_B)^2 + \frac{1}{2} k_C (\bar{d}_C - \bar{z}_C)^2 + \frac{1}{2} k_D (\bar{d}_D - \bar{z}_D)^2
\end{aligned} \tag{2-7}$$

where T represents the kinetic energy and V represents the potential energy of the system. For simplicity, we assume

$$\begin{cases} k_A = k_D = k_f \\ k_B = k_C = k_r \\ c_A = c_D = c_f \\ c_B = c_C = c_r \end{cases} \tag{2-8}$$

Here k is the spring coefficient and c is the damping coefficient of each suspension.

Then we have

$$\begin{aligned}
T &= \frac{1}{2}m\dot{Z}^2 + \frac{1}{2}I_x\dot{\theta}_x^2 + \frac{1}{2}I_y\dot{\theta}_y^2 \\
V &= mg(\bar{Z} - \bar{Z}_0) + \frac{1}{2}k_f((\bar{d}_A - \bar{z}_A)^2 + (\bar{d}_D - \bar{z}_D)^2) + \frac{1}{2}k_r((\bar{d}_B - \bar{z}_B)^2 + (\bar{d}_C - \bar{z}_C)^2) \\
L &= T - V
\end{aligned} \tag{2-9}$$

and the generalized forces can be derived as follows.

$$\begin{aligned}
\bar{Q}_Z &= -c_A(\dot{\bar{d}}_A - \dot{\bar{z}}_A) - c_B(\dot{\bar{d}}_B - \dot{\bar{z}}_B) - c_C(\dot{\bar{d}}_C - \dot{\bar{z}}_C) - c_D(\dot{\bar{d}}_D - \dot{\bar{z}}_D) \\
&= -c_f(\dot{\bar{d}}_A + \dot{\bar{d}}_D - \dot{\bar{z}}_A - \dot{\bar{z}}_D) - c_r(\dot{\bar{d}}_B + \dot{\bar{d}}_C - \dot{\bar{z}}_B - \dot{\bar{z}}_C) \\
\bar{Q}_{\theta_x} &= \frac{w}{2}[-c_A(\dot{\bar{d}}_A - \dot{\bar{z}}_A) - c_B(\dot{\bar{d}}_B - \dot{\bar{z}}_B)] - \frac{w}{2}[-c_C(\dot{\bar{d}}_C - \dot{\bar{z}}_C) - c_D(\dot{\bar{d}}_D - \dot{\bar{z}}_D)] \\
&= -\frac{w}{2}[c_f(\dot{\bar{d}}_A - \dot{\bar{z}}_A - \dot{\bar{d}}_D + \dot{\bar{z}}_D) + c_r(\dot{\bar{d}}_B - \dot{\bar{z}}_B - \dot{\bar{d}}_C + \dot{\bar{z}}_C)] \\
\bar{Q}_{\theta_y} &= \frac{\ell}{2}[-c_B(\dot{\bar{d}}_B - \dot{\bar{z}}_B) - c_C(\dot{\bar{d}}_C - \dot{\bar{z}}_C)] - \frac{\ell}{2}[-c_D(\dot{\bar{d}}_D - \dot{\bar{z}}_D) - c_A(\dot{\bar{d}}_A - \dot{\bar{z}}_A)] \\
&= -\frac{\ell}{2}[-c_f(\dot{\bar{d}}_D - \dot{\bar{z}}_D + \dot{\bar{d}}_A - \dot{\bar{z}}_A) + c_r(\dot{\bar{d}}_B - \dot{\bar{z}}_B + \dot{\bar{d}}_C - \dot{\bar{z}}_C)]
\end{aligned} \tag{2-10}$$

Substituting (2-9) and (2-10) into the Lagrangian equation as follows.

$$\begin{aligned}
\frac{d}{dt}\left(\frac{\partial L}{\partial \dot{Z}}\right) - \frac{\partial L}{\partial Z} &= \bar{Q}_Z \\
\frac{d}{dt}\left(\frac{\partial L}{\partial \dot{\theta}_x}\right) - \frac{\partial L}{\partial \theta_x} &= \bar{Q}_{\theta_x} \\
\frac{d}{dt}\left(\frac{\partial L}{\partial \dot{\theta}_y}\right) - \frac{\partial L}{\partial \theta_y} &= \bar{Q}_{\theta_y}
\end{aligned} \tag{2-11}$$

We obtained the three equations of motion of the ATV.

$$\begin{aligned}
m\ddot{z} + mg + k_f(-\ell\beta + 2z - z_A - z_D) + k_r(\ell\beta + 2z - z_B - z_C) \\
+ c_f(-\ell\dot{\beta} + 2\dot{z} - \dot{z}_A - \dot{z}_D) + c_r(\ell\dot{\beta} + 2\dot{z} - \dot{z}_B - \dot{z}_C) = 0
\end{aligned} \tag{2-12}$$

$$\begin{aligned}
I_x\ddot{\alpha} + \frac{w}{2}[k_f(w\alpha - z_A + z_D) + k_r(w\alpha - z_B + z_C)] \\
+ \frac{w}{2}[c_f(w\dot{\alpha} - \dot{z}_A + \dot{z}_D) + c_r(w\dot{\alpha} - \dot{z}_B + \dot{z}_C)] = 0
\end{aligned} \tag{2-13}$$

$$I_y \ddot{\beta} + \frac{\ell}{2} [-k_f(-\ell\beta + 2z - z_A - z_D) + k_r(\ell\beta + 2z - z_B - z_C)] \\ + \frac{\ell}{2} [-c_f(-\ell\dot{\beta} + 2\dot{z} - \dot{z}_A - \dot{z}_D) + c_r(\ell\dot{\beta} + 2\dot{z} - \dot{z}_B - \dot{z}_C)] = 0 \quad (2-14)$$

The above equations of motion (2-12), (2-13), (2-14) can be rearrange as follows

$$[M]\{\ddot{q}\} + [C]\{\dot{q}\} + [K]\{q\} = [r] \text{ , where } q = \begin{bmatrix} z \\ \alpha \\ \beta \end{bmatrix} \quad (2-15)$$

and the state-space form of the system is written as follows

$$\begin{bmatrix} \dot{q} \\ \ddot{q} \end{bmatrix} = \begin{bmatrix} 0 & I \\ -M^{-1}K & -M^{-1}C \end{bmatrix} \begin{bmatrix} q \\ \dot{q} \end{bmatrix} + \begin{bmatrix} 0 \\ M^{-1} \end{bmatrix} r(t) \\ \begin{bmatrix} q \\ \dot{q} \\ \ddot{q} \end{bmatrix} = \begin{bmatrix} I & 0 \\ 0 & I \\ -M^{-1}K & -M^{-1}C \end{bmatrix} \begin{bmatrix} q \\ \dot{q} \end{bmatrix} + \begin{bmatrix} 0 \\ 0 \\ M^{-1} \end{bmatrix} r(t) \quad (2-16)$$

where

$$M = \begin{bmatrix} m & 0 & 0 \\ 0 & I_x & 0 \\ 0 & 0 & I_y \end{bmatrix} \quad (2-17)$$

$$C = \begin{bmatrix} 2(cf + cr) & 0 & \ell(-cf + cr) \\ 0 & \frac{w^2}{2}(cf + cr) & 0 \\ \ell(-cf + cr) & 0 & \frac{\ell^2}{2}(cf + cr) \end{bmatrix} \quad (2-18)$$

$$K = \begin{bmatrix} 2(kf + kr) & 0 & \ell(-kf + kr) \\ 0 & \frac{w^2}{2}(kf + kr) & 0 \\ \ell(-kf + kr) & 0 & \frac{\ell^2}{2}(kf + kr) \end{bmatrix} \quad (2-19)$$

Equation (2-16) can be used to construct the dynamic model with Simulink. The scheme of Simulink model is shown in Figure 2.2

2.2 Whole body vibration

Whole body vibration is the mechanical vibration (or shock) transmitted to the body as a whole. It is often due to the vibration of a surface supporting the body [11]. The effects of vibration could be subdivided into three main headings, namely (a) interference with comfort, (b) interference with activities and (c) interference with health. Each criterion has different conditions and limits associated with it.

Frequencies below about 0.5Hz may eventually lead to symptoms of motion sickness. Different parts of the body resonate at different frequencies. In the vertical direction resonance starts at about 2Hz, but the first major resonance occurs at about 5Hz. The transmissibility of vertical vibration to the head is sometimes a maximum at 4Hz. The voice may be caused to warble by vibrations between 10Hz and 20Hz. Vision may be affected at any frequency, but blurring occurs between 15Hz and 60Hz. The dominate vibration transmitted through the seats of vehicles is often at frequency below 20Hz [11]. It was thus decided to limit the investigation to frequencies below 20Hz.

Comfort is more difficult to determine since it is subjective and has a lot to do with the psyche. It is important to note that frequency and not only amplitude contribute to the perception of comfort. An experiment done by Fothegrill and Griffin in 1977 showed that for a seated person excited by a 10Hz sinusoidal vibration for RMS values below 0.4 m/s^2 it was noticeable,

but not uncomfortable. A level of 1.1 m/s^2 was considered to be mildly uncomfortable, 1.8 m/s^2 uncomfortable and RMS values above 2.7 m/s^2 as very uncomfortable.

Most researchers agree that seated humans have a vertical vibration natural frequency at about 4 to 6Hz and a horizontal vibration natural frequency at about 1 to 2Hz. In this frequency ranges the seat motion is most easily transmitted to the upper parts of the body and is not just confined to the area of the body close to the source of vibration [12].

2.3 Legislation

WBV exposures are to be determined separately for the three axes in accordance with ISO 2631-1:1997. Gallais found that comfort is time dependent and suggested that time dependency curves should be incorporated in the evaluation of WBV. ISO 2631 of 1997 doesn't compensate for time dependency of comfort. It was noted that such dependency curves were included in the ISO of 1974, but was since removed.

Up to date there has been much debate about whether the VDV measurements should be used to evaluate WBV on seated humans. The arguments for and against the VDV measurements are usually that it is better at indicating the presence of peaks which tend to be more harmful to humans, but is also more sensitive to human induced motion such as shuffling [13].

VDV is based on the fourth power of acceleration and is therefore more sensitive to shocks compared to the RMS (root mean square) magnitude (ISO 2631-1:1997). The general formula for VDV is

$$VDV_z = \left[\frac{T_s}{N} \sum_{n=1}^N a_w^4 \right]^{1/4} \quad (2-20)$$

with T_s the measured time, N the number of points and a_w the frequency weighted acceleration data. This parameter is time dependent and gives an objective measure of the amount of vibrations a person had to experience with a certain period.

VDV is used as an index of vertical vibration. Besides, the RMS angular velocity is used in this paper as the index of rotation vibration. The general form for RMS angular velocity is

$$J_\alpha = \left[\frac{T_s}{N} \sum_{n=1}^N \dot{\alpha}_w^2 \right]^{1/2} \quad (2-21)$$

$$J_\beta = \left[\frac{T_s}{N} \sum_{n=1}^N \dot{\beta}_w^2 \right]^{1/2} \quad (2-22)$$

with T_s the measured time, N the number of points and $\dot{\alpha}, \dot{\beta}$ the frequency weighted acceleration data. The reason of frequency weighting is that human body is more sensitive to certain vibration frequency and is described as follows.

The perception and influence of whole body vibration in humans is strongly dependent on the direction, magnitude and frequency of the vibration exposure. From the literature review it was seen that seated humans have a vertical resonance at about 4-6Hz and a horizontal resonance at about 1-2Hz [11]. At these frequencies the motion of the seat

is transferred most easily to the upper parts of the body. Frequency weightings are applied to the acceleration data. The frequency weightings are designed to not affect those frequencies where the body is most sensitive and to attenuate at those frequencies where the response of the body is less sensitive. In principle, weightings do not amplify at any frequency. Although there are problems with the use of the frequency weightings, there are currently no alternative methods of assessment.

A couple of weightings curves (filters) are specified by ISO 2631:1997 depending on the orientation of the person and the direction of vibration. For a seated person the W_k curve is used to weigh the frequency contribution for vertical vibrations and the W_d curve is used to weigh the frequency contribution for lateral vibrations [12]. The frequency weighting curves are shown in Figure 2.3 [16]. The black line represents the W_k weighting curve and the blue one represents the W_d weighting curve. The lateral axis is frequency represented in log scale and the vertical axis is magnitude represented in log scale, too. The idea of the frequency weighting curve is to attenuate the magnitude of acceleration (or velocity) whose frequency lies outside the human resonance frequency. For vertical vibration, the frequency weighting curve is W_k which attenuates the magnitude whose frequency doesn't lie between 4 and 6 Hz. For lateral vibration, the frequency weighting curve is W_d which attenuates the magnitude whose frequency doesn't lie between 1 and 2 Hz.

Assessments are made independently in each direction. Figure 2.4 shows which weighting curve should be applied to which axis [16]. For lateral vibration, the weighting curve is W_d and for vertical vibration, the weighting curve is W_k . A second order shaped curve of the form

$$H_k(s) = \frac{50s + 500}{s^2 + 50s + 1200} \quad (2-23)$$

has been used in [13, 14] to approximate the ISO weighting curve W_k and shown in Figure 2.5. Another second order shaped curve of the form

$$H_d(s) = \frac{9s + 20}{s^2 + 10s + 40} \quad (2-24)$$

has been used to approximate the ISO weighting curve W_d and shown in Figure 2.6.



Chapter 3 Suspension optimization

3.1 History of Genetic algorithm

Computer simulations of evolution started in 1954 with the work of Nils Aall Barricelli. From this beginning, computer simulation of evolution by biologist became more common in the early 1960s. Artificial evolution became a widely recognized optimization method as a result of the work of Ingo Rechenberg in the early 1970 – his group was able to solve complex engineering problems through evolution strategies. GA in particular became popular through the work of John Holland, especially his book in 1975. Research in GA remained largely theoretical until the mid-1980s, when the first International Conference on Genetic Algorithm was held at the University of Illinois.

Genetic Algorithm (GA) or Evolutionary Algorithm (EA) is applied to the optimization of the suspension parameters in this paper. GA is computer-based techniques that mirror natural genetic evolution, and they have been found to be successful in application to a wide range of problems that are difficult to solve analytically. GA is categorized as global search heuristics, and use techniques inspired by evolutionary biology such as inheritance, selection, crossover, and mutation. Comparing with the gradient-based optimization methods, GA needs no derivative information and can deal with a large number of parameters. Besides, GA searches from a wide sampling of the cost surface simultaneously. Figure 3.1 shows the gradient-based optimization algorithm and Figure 3.2 shows the GA-based algorithm.

The evolution search usually starts from a population of randomly generated individuals and happens in generations. In each generation, the fitness of every individual in the population is evaluated, multiple individuals are stochastically selected as parents from the current population (based on their fitness) to proceed crossover, and some of the offspring are randomly mutated. Then the selected parents and offspring construct the new population used in the next iteration of algorithm. The scheme of the procedure of GA is shown in Figure 3.3. [8].

In this paper, the programming of GA is written using MATLAB and combined with the ATV model build with simulink. Each part of the program will be introduced in next paragraph briefly.

3.2 GA procedures

The genetic algorithm program contain following parts: initial population, cost evaluation, mate selection, crossover and mutation [16]. Each part of above will be stated as follows.

3.2.1 Initial population

The initial population is generated randomly between the upper and lower bounds of parameters.

$$IPOP = (hi - lo) \times random\{N_{pop}, N_{par}\} + lo \quad (3-1)$$

where $random\{N_{ipop}, N_{par}\}$ is a function that generates an $N_{pop} \times N_{par}$ matrix of uniform random numbers between zero and one, hi is the highest value in the parameter range and lo is the lowest value in the parameter range.

In our problem, each individual in the population contains two parameters, spring coefficient k and damping coefficient c , which values are chosen according the constraint functions. The size of initial population N_{pop} and numbers of generations will both affect the time cost of computation. The recommend size of initial population and numbers of generations are 40 and 100.

3.2.2 Cost evaluation

Mathematical optimization is the process of the formulation and then the solution of a constrained optimization problem of the general mathematical form:

$$\begin{aligned}
 & \text{minimize or maximize } f(x), x = (x_1, x_2, \dots, x_n) \in R^n \\
 & \text{subject to constrains} \\
 & g_i(x) \leq 0, \quad j = 1, 2, \dots, m \\
 & h_j(x) = 0, \quad j = 1, 2, \dots, r < n
 \end{aligned} \tag{3-2}$$

where $f(x)$, $g_j(x)$ and $h_j(x)$ are scalar function of x . The components of x are called the design variables, $f(x)$ the objective function or cost function and $g_j(x)$ and $h_j(x)$ are respectively referred to as the inequality and equality constraint functions.

The formulation of the optimization problem requires identifying the cost function, the variables and the constraints. In our optimization problem, the variables are the spring coefficient k and damping coefficient c . The constraints are inequality functions which limit the upper and lower bounds of k and c .

Two competing goals are consider here: one is the comfort which is numerical presented by VDV and RMS angular velocity described in last

chapter, and the other is the rattle-space limit. A kind of fitness measure, φ , that penalize controls that pass too close the rattle-space limits [15]. The penalty function is shown in Figure 3.4 and written of the form

$$\varphi(\Delta z) = \begin{cases} e^{(|\Delta z| - m_1)} - 1, & |\Delta z| > m_1 \\ 0 & , |\Delta z| < m_1 \end{cases} \quad (3-3)$$

where $\Delta z = Z - Z_i$, $i = A, B, C, D$, see Figure 2.1. m_1 and m_2 are parameters which are used to penalize a suspension that is too close to its rattle space limits. At a distance of $m_1 + m_2$ it has reached its safety limit; within a distance of m_1 it is inside the safe travel limit. The summation of φ , equation (3-4), is used to indicate the extent to which the system stays within the limits of the rattle space during a simulation.

$$\sum_{n=1}^N \varphi(\Delta z) \quad (3-4)$$

Thus, the two fitness measure used in the optimization was a weighted sum of the measures in equation (2-20) and (3-3), as shown in equation (3-5) below. The change in outcomes can be compared as the weighting, λ , is varied from zero to one.

$$\text{cost function} = \lambda \left(\left[\frac{T_s}{N} \sum_{n=1}^N a_w^4 \right]^{1/4} + \left[\frac{T_s}{N} \sum_{n=1}^N \dot{\alpha}_w^2 \right]^{1/2} + \left[\frac{T_s}{N} \sum_{n=1}^N \dot{\beta}_w^2 \right]^{1/2} \right) + (1-\lambda) \sum_{n=1}^N \varphi(z) \quad (3-5)$$

with T_s the measured time, N the number of points and a_w the frequency weighted acceleration data.

Fitness of each individual of the initial population is calculated using the cost function, equation (3-5) and is sorted in descending order. That is, the smaller value will have better fitness.

3.2.3 Mate selection

The selection of mate is according to the fitness of each individual. The better the “gene” is, the higher the possibility of be preserved. The mate selection method used in this paper is the roulette wheel selection. Here we defined the *xfitness* which equals fitness of each individual divided by the sum of all fitness of the population. Therefore, the comparison table can be created by the cumulative probability. The MATLAB code is as follows

```
xfitness = fitness/sum(fitness); % Roulette wheel selection  
cum_probability = cumsum(xfitness); % Comparison table created
```

Selection of mate is to create a random value varied form one to zero and choose the first individual whose *xfitness* is larger than the random value. Repeating the selection procedure, the chosen parents will proceed with the crossover.



3.2.4 Crossover and Mutation

Parents selected above reproduce offspring through the crossover procedure. Kinds of method for crossover were developed and the single point crossover is used here because of the numbers of parameters. The single point crossover means the parameters before crossover point exchanged and the parameters after crossover point mixed using following equation.

$$\begin{aligned} p_{new1} &= p_1 - \mu[p_1 - p_2] \\ p_{new2} &= p_2 + \mu[p_1 - p_2] \end{aligned} \quad (3-6)$$

where μ is varied form zero to one. The crossover procedure is illustrated in Figure 3.5. After crossover, comes the mutation. A mutate rate between 1

and 8 % often works well. Number of mutate parameters is decided through equation (3-7)

$$N_{mut} = mutate_rate * N_{pop} * N_{par} \quad (3-7)$$

where N_{mut} is the number of mutate parameters. The mutation is, for example, if N_{mut} equals two then two parameters of the offspring are replaced by new values which are generated randomly between the parameters constraints.

By producing offspring using the above methods of crossover and mutation, a new solution is created which typically shares many of the characteristics of its "parents". New parents are selected for each offspring, and the process continues until a new population of solutions of appropriate size is generated. These processes ultimately result in the next generation population of parameters that is different from the initial generation.

Generally the average fitness will have increased by this procedure for the population, since only the best individuals from the first generation are selected for mating. This generational process is repeated until a termination condition has been reached. Common terminating condition is when a fixed number of generations reached.

3.3 Optimization of passive suspension

The passive suspension systems consist of the passive components spring and oil damper. When the vehicle bumped along the rough road, the work of suspension system is to absorb energy and reduce the vibration. Since the spring coefficient k and damping coefficient c of passive suspension were fixed and untunable during driving, the preset of k and

c is important for the comfortable and vehicle handling. In order to find the appropriate value of k and c for certain road condition, our scheme is showed in Figure 3.6. For passive suspension system, we first collect certain road profiles as the inputs \bar{Z}_A , \bar{Z}_B , \bar{Z}_C , \bar{Z}_D . Then we collect the acceleration data of ATV and through the optimization procedure introduced above, the optimized k and c will be suit to this road condition. Different road profiles result in corresponding different setting of k and c . We call this procedure an *offline* design method.



Chapter 4 Simulation result

4.1 Road profile data

The road profile data is collected from an ATV driving simulation game made by IMON corp. The game contains kinds of different road conditions including loess, timberland, highway, sand beach and jouncing areas. When player driving ATV on these areas, the setting of suspension parameters k and c will affect the feeling of the whole body vibration transferred from the road. In order to improve the comfort of driver for different road conditions, we use the road profile data as inputs \bar{Z}_A , \bar{Z}_B , \bar{Z}_C , \bar{Z}_D , then proceed the optimization procedure to find the optimized values of k and c .

Two kinds of road profiles were used here and the left and right road profiles which pass through A, B and C, D are similar but not the same. Road profile one is jouncing road with a 35 centimeters high-low variation and higher bump frequency. The number of data points is 3180, and sampling period is 0.005 seconds. The graph is shown in Figure 4.1 and Figure 4.2 which represent the road profiles pass through left and right of ATV, respectively. Road profile two is mild road with a 10 centimeters high-low variation and lower bumping frequency. The number of data points is 2900, and sampling period is 0.005 seconds. The graph is shown in Figure 4.3 and Figure 4.4 which similarly represent left and right road profiles, respectively.

4.2 Optimization results

The ATV model used here is HONDA TRX250EX Sport ATV with specifications listed in Table 4.1. The suspension system is made by DNM Suspension with adjustable spring and damper design for ATV using. The default setting of suspension parameters is $k = 22000 N/m$ and $c = 1200 N s/m$. Before optimization, the setting of genetic algorithm is listed in Table 4.2 and the limit constraints of k and c are $10000 < k < 25000$ and $1000 < c < 2500$.

Simulation one is using road profile one shown in Figure 4.1 and Figure 4.2 as the inputs from ground to wheels A, B and C, D. The optimized $k = 14480.6587 N/m$ and $c = 1002.6731 N/m$. The optimized weighted vertical acceleration \ddot{z} is shown in Figure 4.5 with VDV_z attenuated from 16.8403 to $13.6141 m/s^{1.75}$. The blue line is the response of vertical acceleration with optimized k and c , the red line is the response with k and c before optimized. The zoom in of Figure 4.5 is shown in Figure 4.6. In Figure 4.6, the attenuation of weighted vertical acceleration is obviously.

The optimized weighted roll velocity $\dot{\alpha}$ is shown in Figure 4.7 with J_α attenuated from 0.5442 to $0.5341 rad/s^{0.5}$. The zoom in of Figure 4.7 is shown in Figure 4.8. The maximum value of weighted roll velocity shown in Figure 4.8 attenuate from 0.55 to $0.5 rad/s^{0.5}$.

The optimized weighted pitch velocity $\dot{\beta}$ is shown in Figure 4.9 with J_{β} attenuated from 0.3838 to 0.3765 $rad/s^{0.5}$. The zoom in of Figure 4.9 is shown in Figure 4.10. The maximum value of weighted pitch velocity shown in Figure 4.10 attenuate from 0.31 to 0.28 $rad/s^{0.5}$.

The fitness of genetic algorithm is shown in Figure 4.11. The lateral axis is generation and the vertical .the best generation occurred at number 90.

Simulation two is using road profile two shown in Figure 4.3 and Figure 4.4 as the inputs from ground to wheels A, B and C, D. The optimized $k = 12503.0626 N/m$ and $c = 1009.9273 N/m$. The optimized weighted vertical acceleration \ddot{z} is shown in Figure 4.12 with VDV_z attenuated from 4.28 to 3.4457 $m/s^{1.75}$. The blue line is the response of vertical acceleration with optimized k and c , the red line is the response with k and c before optimized. The zoom in of Figure 4.12 is shown in Figure 4.13. In Figure 4.13, the attenuation of weighted vertical acceleration is obviously.

The optimized weighted roll velocity $\dot{\alpha}$ is shown in Figure 4.14 with J_{α} attenuated from 0.0976 to 0.0921 $rad/s^{0.5}$. The zoom in of Figure 4.14 is shown in Figure 4.15. The minimum value of weighted roll velocity shown in Figure 4.15 attenuate from -0.11 to -0.09 $rad/s^{0.5}$.

The optimized weighted pitch velocity $\dot{\beta}$ is shown in Figure 4.16 with J_{β} attenuated from 0.0878 to 0.0841 $rad/s^{0.5}$. The zoom in of Figure 4.16 is shown in Figure 4.17. The maximum value of weighted pitch

velocity shown in Figure 4.17 attenuate from 0.095 to 0.085 $rad / s^{0.5}$.

The fitness of genetic algorithm is shown in Figure 4.18. The lateral axis is generation and the vertical .the best generation occurred at number 96.

The optimization results of road profile one and road profile two are listed in Table 4.3 and Table 4.4.

4.2 Discussion

The optimization results of road profile one and road profile two show that the GA can efficiently converge to the optimal solution. In the process of optimization, the number of generation that GA converges to the optimal solution is not fixed. Theoretically, the more the number of generations the better the fitness is. In our simulation, the number of generations is fixed to 100, so that the GA will automatically stop when the number of generations reaches 100. After many times of simulation, 100 generations are considered that suitable as the stop condition.

The optimization results also show that the optimized suspension spring coefficient k and damping coefficient c can effectively attenuated vibration transmitted from road inputs. The optimization data reveals that for road profile one, after optimization VDV_z has an improvement of 19.16%, $\dot{\alpha}$ has an improvement of 9.09% in maximum value and $\dot{\beta}$ has an improvement of 9.68% in maximum value. For road profile two, after optimization VDV_z has an improvement of 19.49%, $\dot{\alpha}$ has an improvement of 18.18% in minimum value and $\dot{\beta}$ has an improvement of

10.53% in maximum value.

The GA is one of global optimization methods. In this study, our simulation data reveal that GA is suitable for the optimization design for ATV suspension parameters and indeed reduce the VDV_z , J_α and J_β . The response of weighted vertical acceleration, weighted roll velocity and weighted pitch velocity are also improved after optimization.



Chapter 5 Conclusion

The main purpose of this study is to establish a series of optimization procedure to find the appropriated setting of passive suspension parameters k and c . The spring coefficient k and damping coefficient c of passive suspension are unchangeable during driving. Thus, in order to attenuate vibration transmitted from road roughness and improve the comfort of drivers, a global optimization algorithm, genetic algorithm, was used in this paper.

A full-car model of ATV with three degree-of-freedom z , α and β which represent the vertical displacement, roll angle and pitch angle respectively was derived in this study. The vibration dose value (VDV) and RMS angular velocity are calculated and used as the assessments of discomfort of human body.

Two kinds of road profiles with different high-low variation and bumping frequency were used as the road inputs. Results of simulation one and two show that the VDV_z , J_α and J_β are reduced which means the vibrations transmitted from road to human body are attenuated and the optimized k and c are found. The results of simulations reveal that the genetic algorithm is effective to optimize passive suspension parameters and improve the comfort of driver.

There are some advantages of using of genetic algorithm. First, GA can deal with large number of parameters. Second, GA doesn't require derivative information. Third, GA can simultaneously search from a wide

sampling of the cost surface. There is also disadvantage of using genetic algorithm that when dealing with large number of road data points and generations, it takes time to find the optimized solution. For this reason, this algorithm is suit for offline optimization but not for online optimization

In this study the consideration of ATV performance indexes focused on the comfort and working space of suspension but not on vehicle handling. The assessment of vehicle handling can be calculated using equation (5-1)

$$J = \frac{1}{T} \int_0^t F_w(t) dt \quad (5-1)$$

where F_w is the force developed between the wheel and the ground [2].



Reference

- [1] Gillespie, T. D. Fundamental of Vehicle Dynamics, Society of Automotive Engineering, Warrendale, PA, 1992.
- [2] G.Verros, S. Natsiavas, C. Papadimitriou, “Design Optimization of Quarter-car Models with Passive and Semi-active Suspensions under Random Road Excitation”, Journal of vibration and control, 11:581-606, 2005.
- [3] Savaresi, S. M., Silani, E., Bittanti, S. And Porciani, N. “Decision and Control”, Proceedings 42nd IEEE Conference, Vol.3, pp.2264-2269, 2003
- [4] Wu, Y. and Xu, B. “Vehicle Electronics Conference”, Proceeding of the IEEE International, Vol. 1, pp.66-69 Changchun, China, 1999
- [5] Hashiyama, T., Furuhashi, T. and Uchikawa, Y. “Evolutionary Computation”, IEEE international Conference, Vol. 1, pp.279, 1995
- [6] Depez, K., Maertens, K., and Ramon, H. “American Control Conference”, Proceeding of the 2002, Vol. 2, pp.1947-1501, 2002
- [7] Bourmistrova, A., Storey, I., Subic, A. “Multiobjective Optimization of Active and Semi-Active Suspension Systems with Application of Evolutionary Algorithm”, RMIT Business Information Systems, RMIT Mechanical and Aerospace Engineering,
- [8] Niahn-Chung Shieh, Chun-Liang Lin, Yu-Chen Lin, Kuo-Zoo Liang, “Optimization design for passive suspension of a light rail vehicle using constrained multi-objective evolutionary search”, Journal of Sound and Vibration, 285, pp.407-424, 2005
- [9] A.F. Naude, J.A. Snyman, “Optimization of road vehicle passive suspension systems. Part 1. Optimization algorithm and vehicle model”,

Applied Mathematical Modeling, 27, pp.249-261, 2003

[10] A.F. Naude, J.A. Snyman, “Optimization of road vehicle passive suspension systems. Part 2. Qualification and case study”, Applied Mathematical Modeling, 27, pp.263-274, 2003

[11] Griffin, G.J., Rakheja, S., Sankar, S., Afework, Y. “Increased comfort and safety of drivers of off-highway vehicles using optimal seat suspension”, SAE Trans, 99, Sec 2, pp.541-548, 1990.

[12] International Organization for Standardization, ISO 2631-1. “Mechanical vibration and shock - Evaluation of Human Exposure to Whole-Body-Vibration. Part 1: General Requirements”. 1997

[13] Elbeheiry, E.M., Karmopp, D.C., Elaraby, M.E. and Abdelraouf, A.M. “Suboptimal Control Design of Active and Passive Suspensions Based on a Full Car Model”. Vehicle System Dynamics, 26, pp.197-222, 2006

[14] Elmandany, M.M. “A procedure for Optimization of Truck Suspensions”. Vehicle System Dynamics, 16, pp.297-312, 1987

[15] Lin, J.-S and Kanellakopoulos, J. “American Control Conference”, Proceeding of the 1997, Vol. 1, pp.714-718, 1997

[16] J. C. Kirstein. “Suspension System Optimization to Reduce Whole Body Vibration Exposure on an Articulated Dump Truck”. Department of engineering, Stellenbosch University, 2005

[17] 周鵬程，遺傳算法原理與應用，三版，全華，台北，2005

Figures



Figure 1.1 Honda TRX250EX Sport ATV

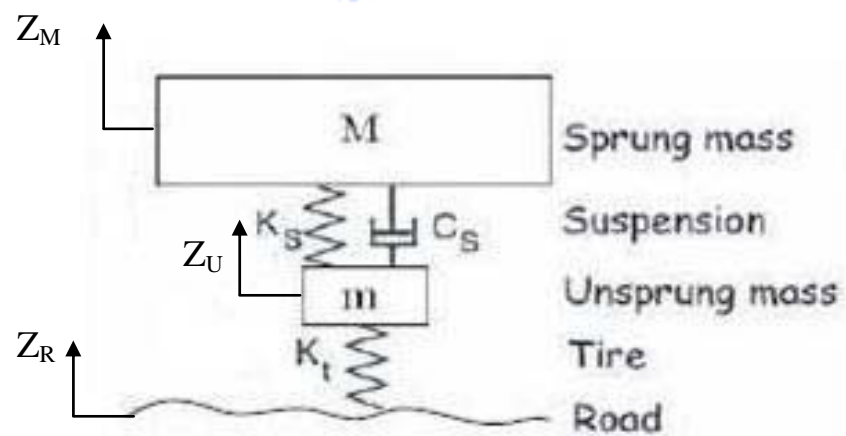


Figure 1.2 Passive suspension systems

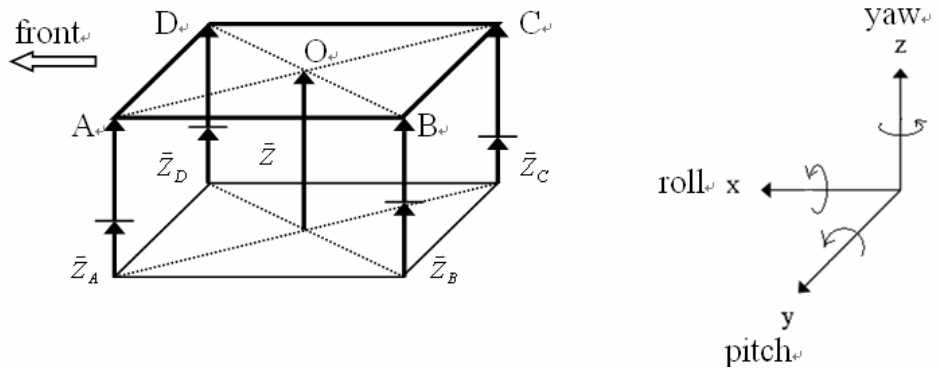


Figure 2.1 Full-car model of ATV

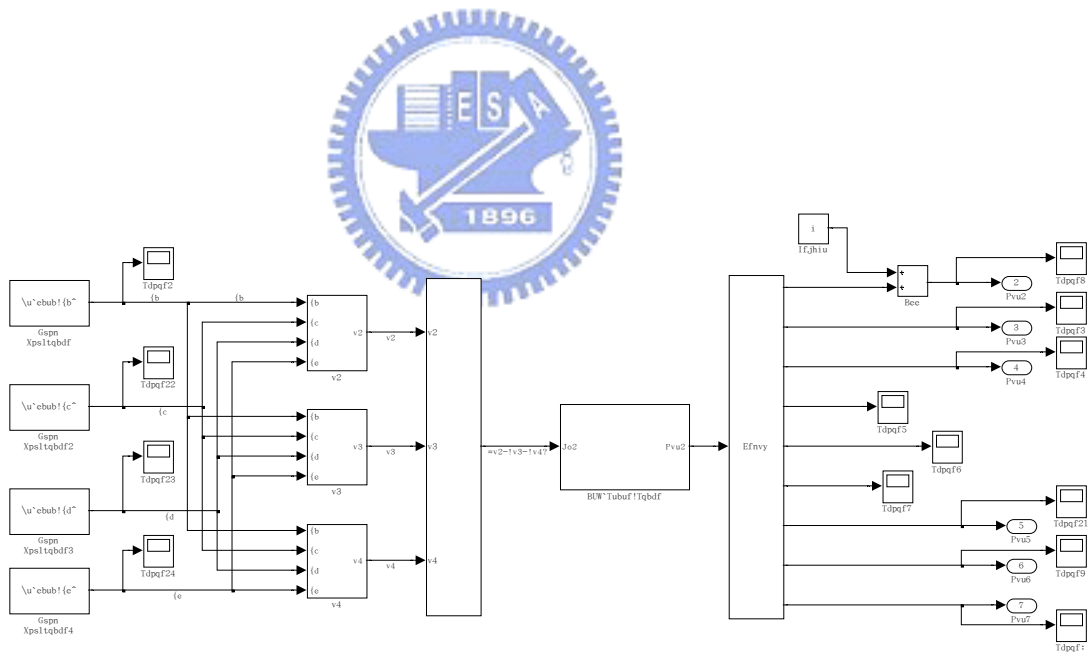


Figure 2.2 simulink model of ATV

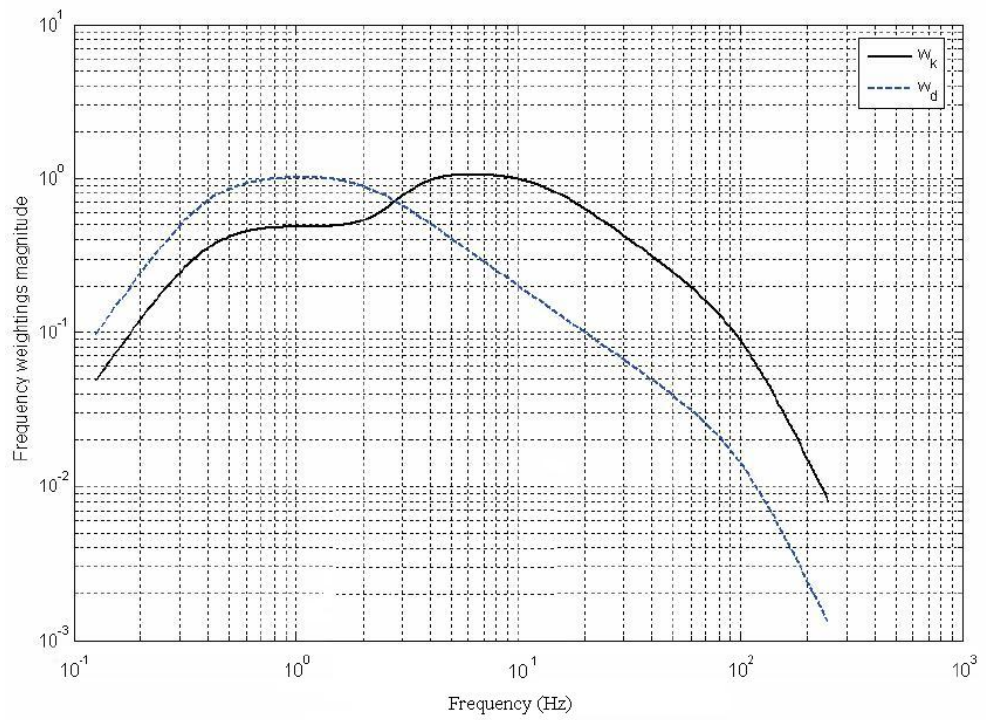


Figure 2.3 Frequency weighting curves (Kirstein 2004)



Weighting filter:

X-axis: ISO 2631-1 W_d

Y-axis: ISO 2631-1 W_d

Z-axis: ISO 2631-1 W_k

Figure 2.4 Axes and weighting curves (Kirstein 2004)

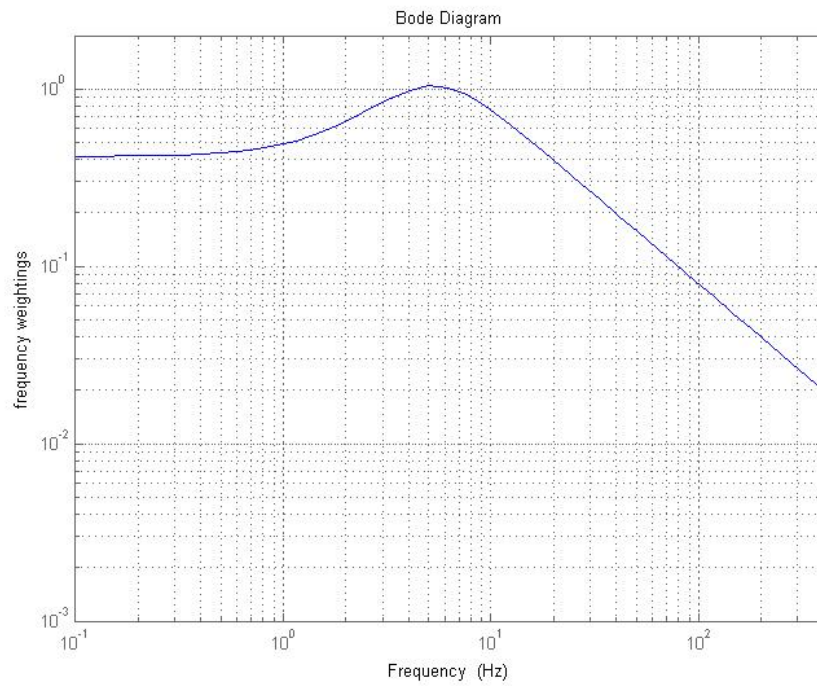


Figure 2.5 Approximate weighting curve of W_k

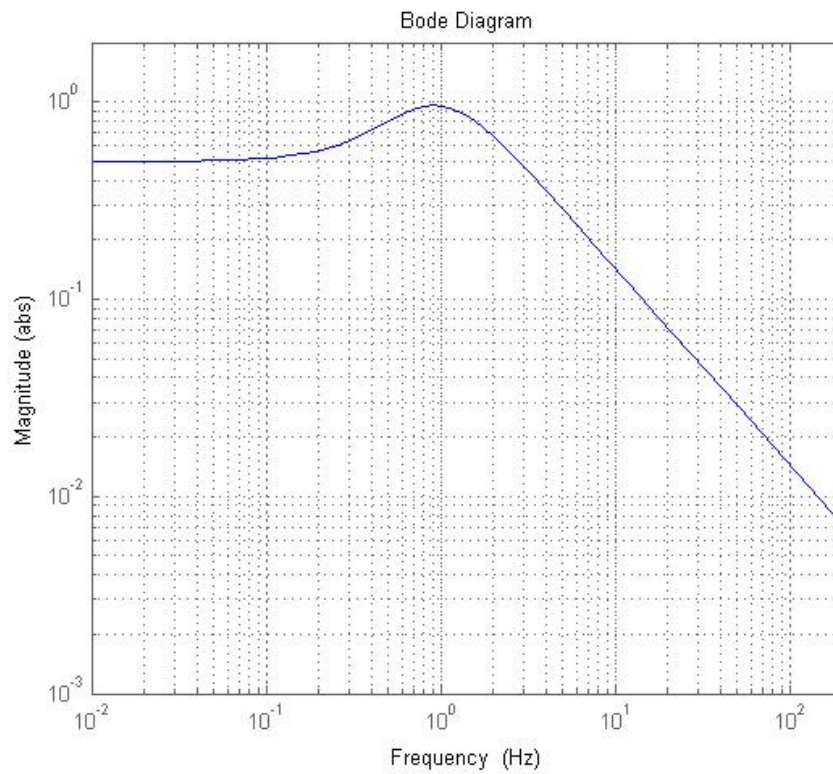


Figure 2.6 Approximate weighting curve of W_d

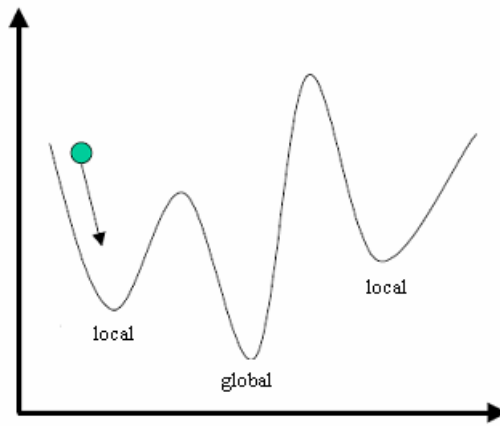


Figure 3.1 gradient-based optimization algorithms

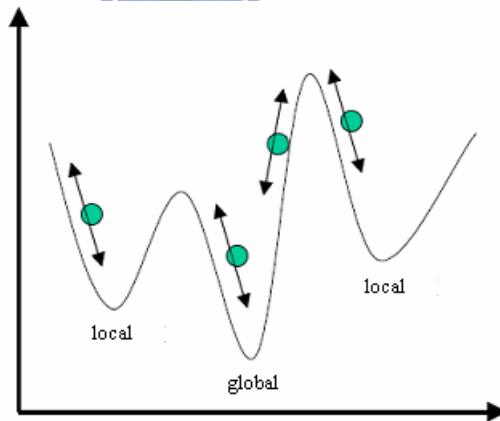


Figure 3.2 GA-based optimization algorithms

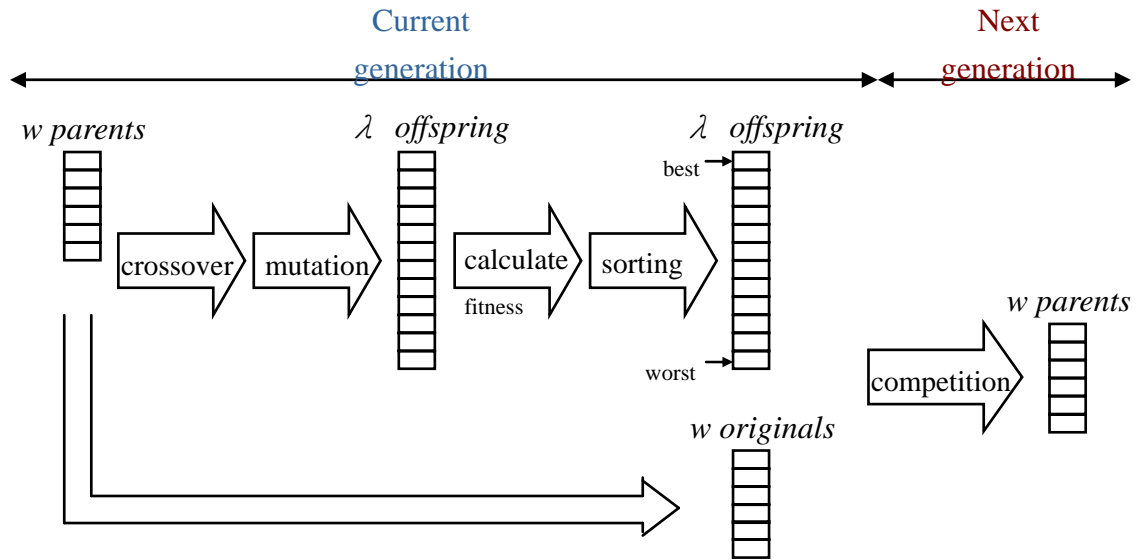


Figure 3.3 the scheme of procedure of GA (Niahn-Chung Shieh, 2005)

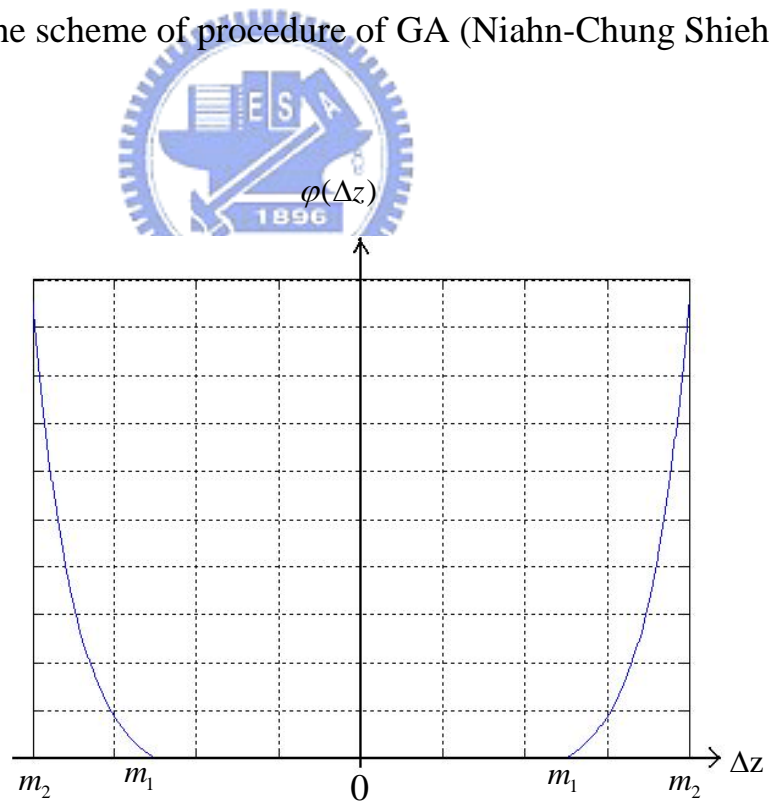


Figure 3.4 the penalty function of rattle space of suspension

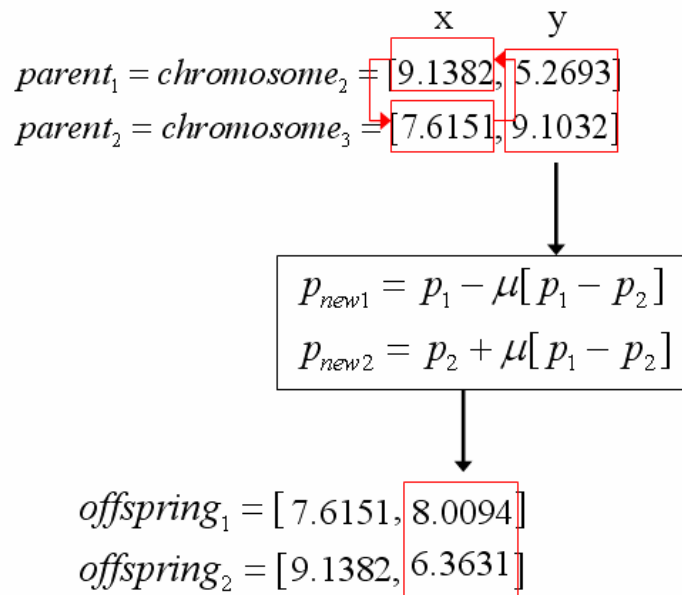


Figure 3.5 illustration of crossover procedure

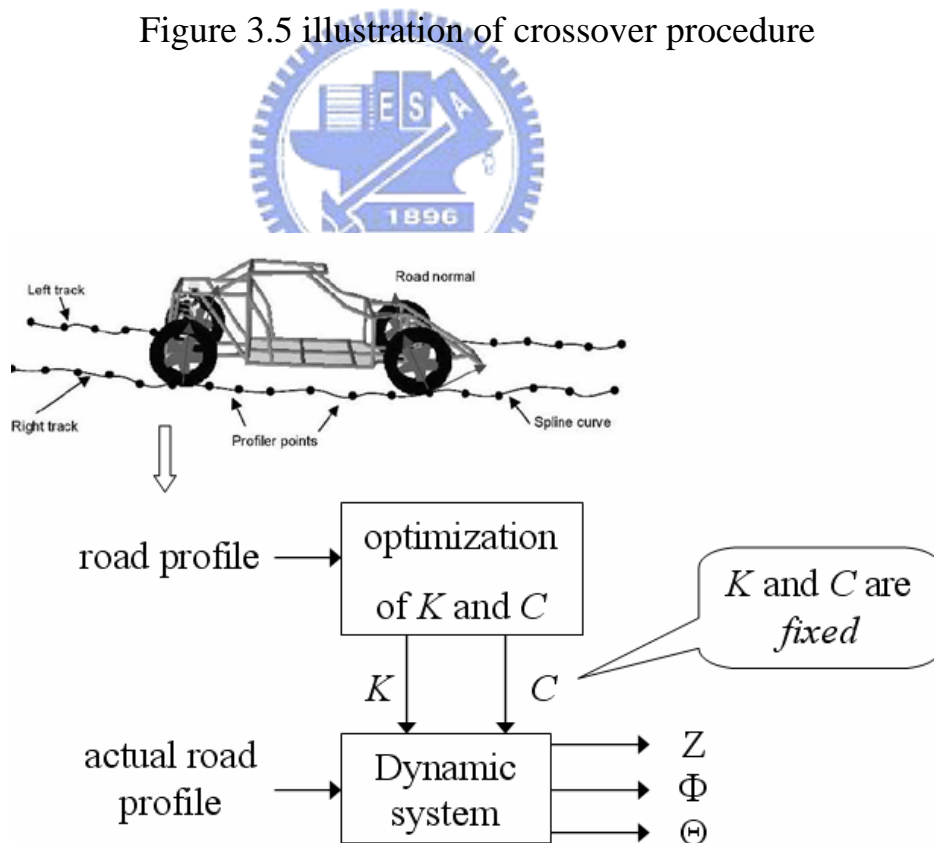


Figure 3.6 scheme of optimization for passive suspension

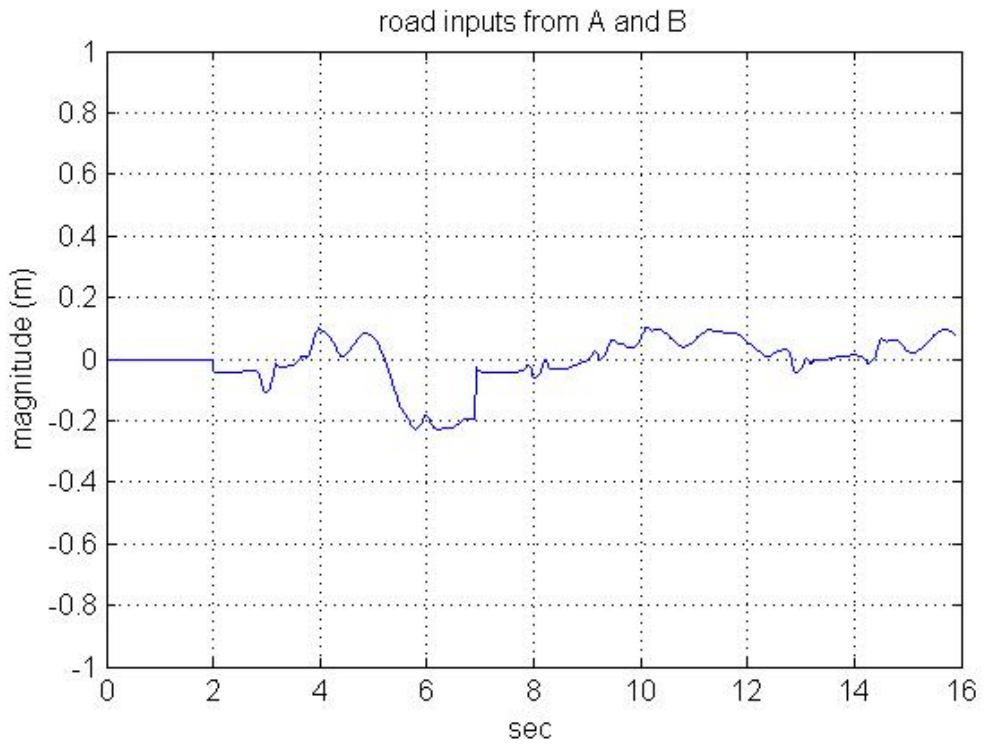


Figure 4.1 road profile one input from A and B

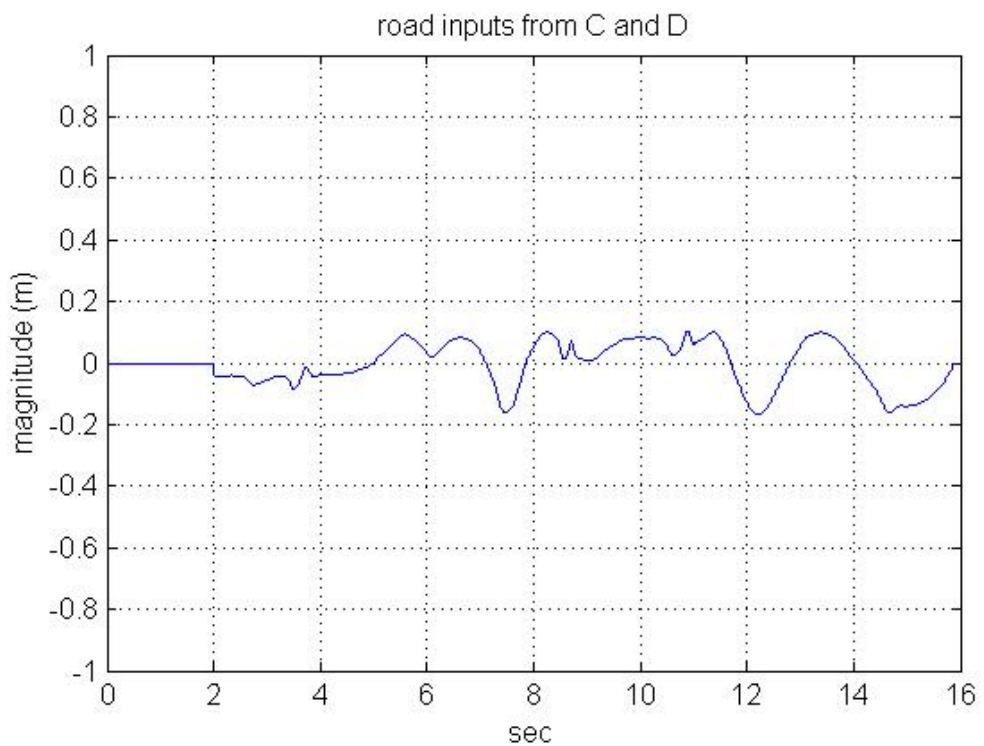


Figure 4.2 road profile one input from C and D

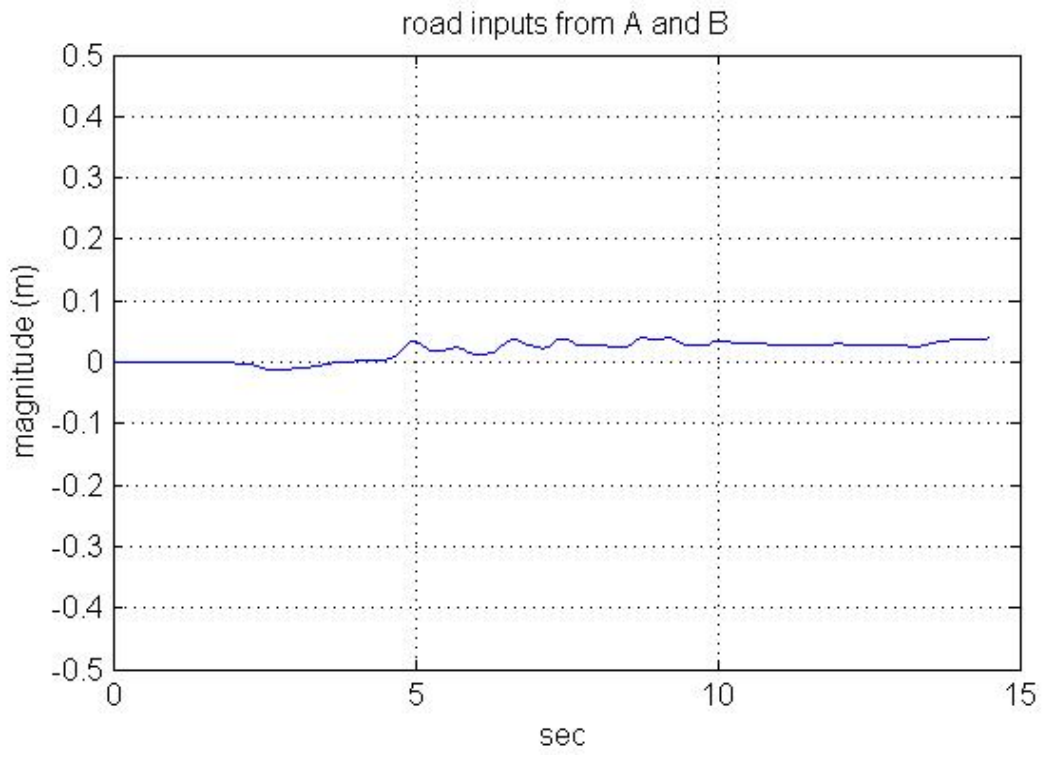


Figure 4.3 road profile two input from A and B

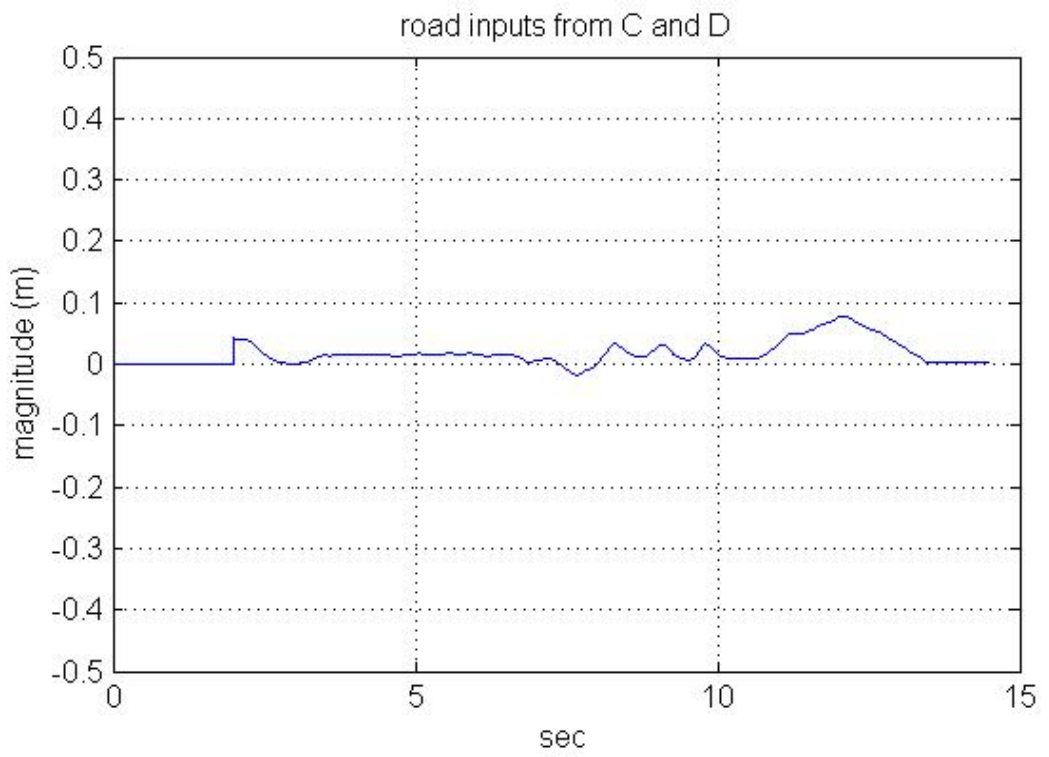


Figure 4.4 road profile two input from C and D

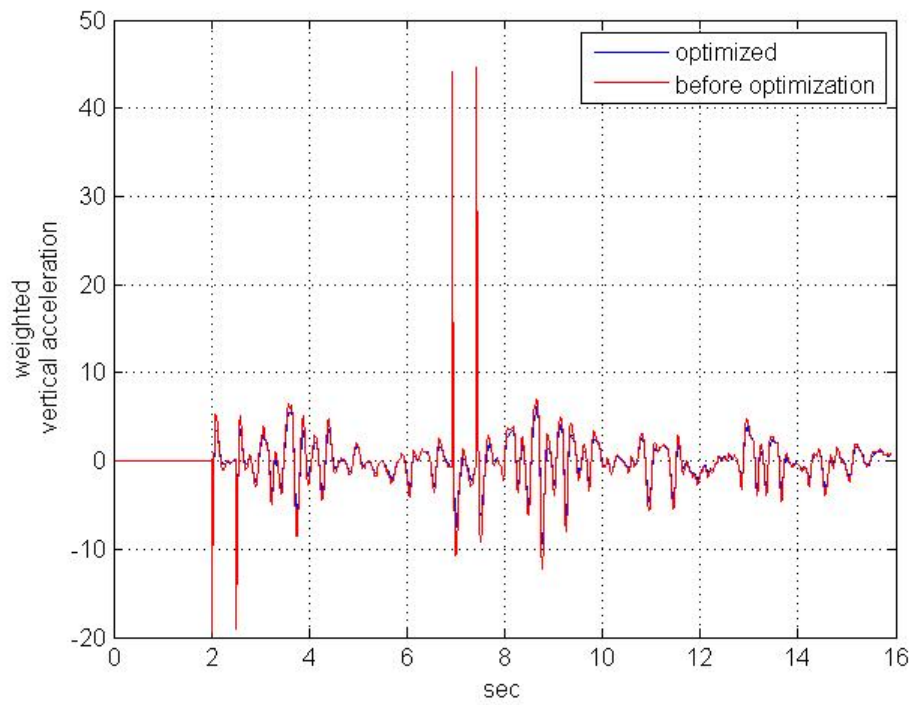


Figure 4.5 optimized weighted vertical acceleration \ddot{z} for road profile one

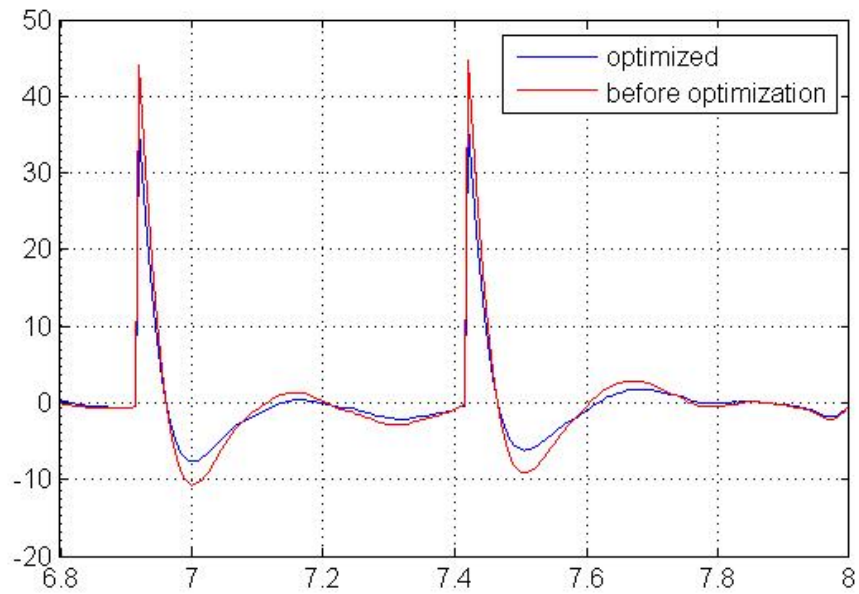


Figure 4.6 optimized weighted vertical acceleration \ddot{z} for road profile one
between 6.8 and 8 sec

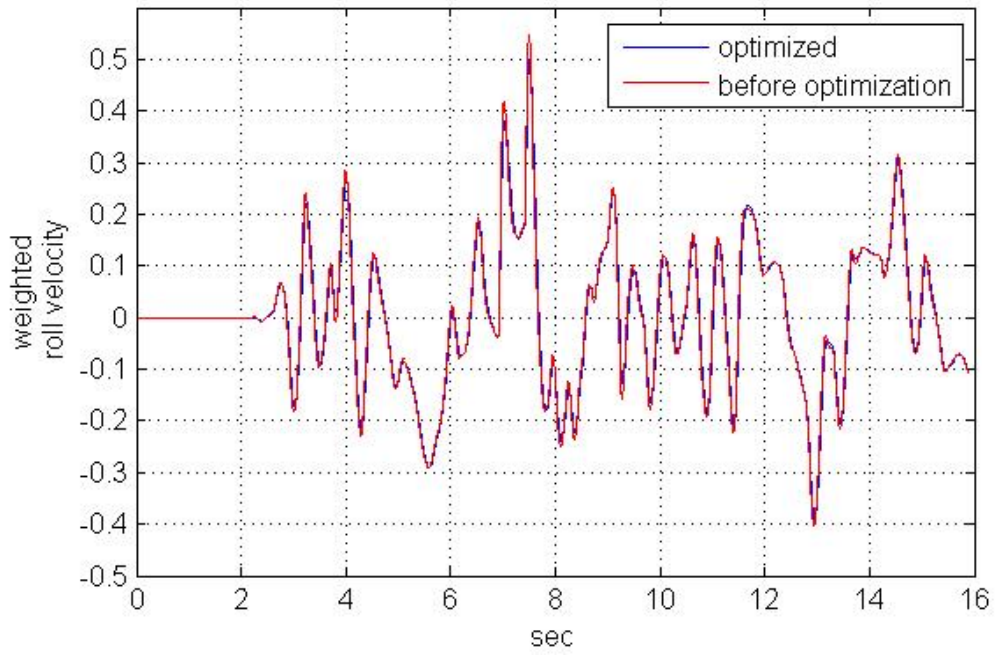


Figure 4.7 optimized weighted roll velocity $\dot{\alpha}$ for road profile one

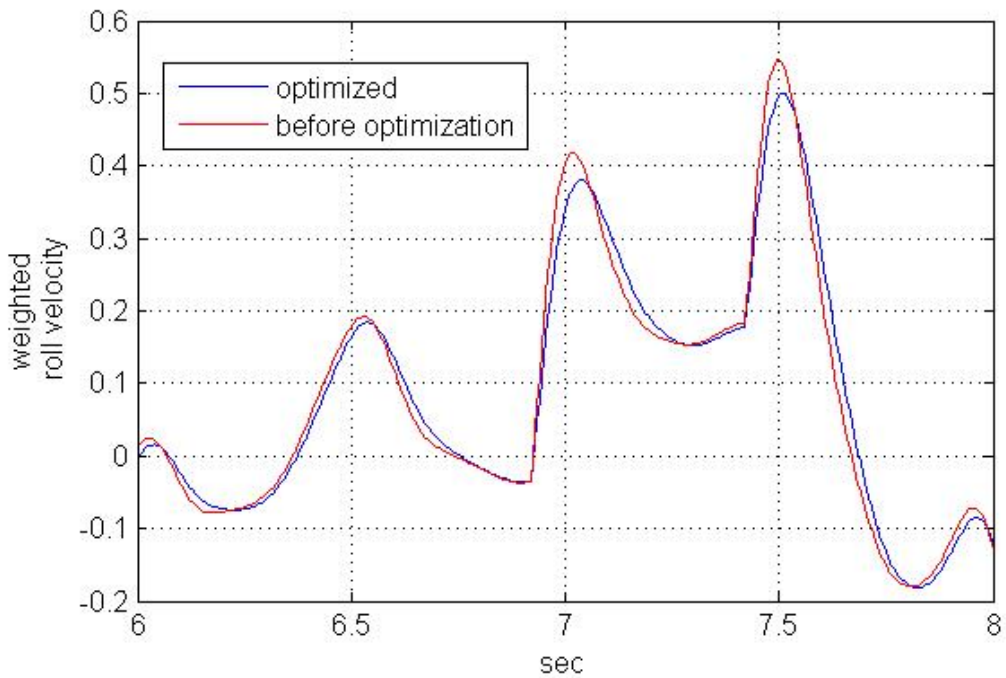


Figure 4.8 optimized weighted roll velocity $\dot{\alpha}$ for road profile one between 6 and 8 sec

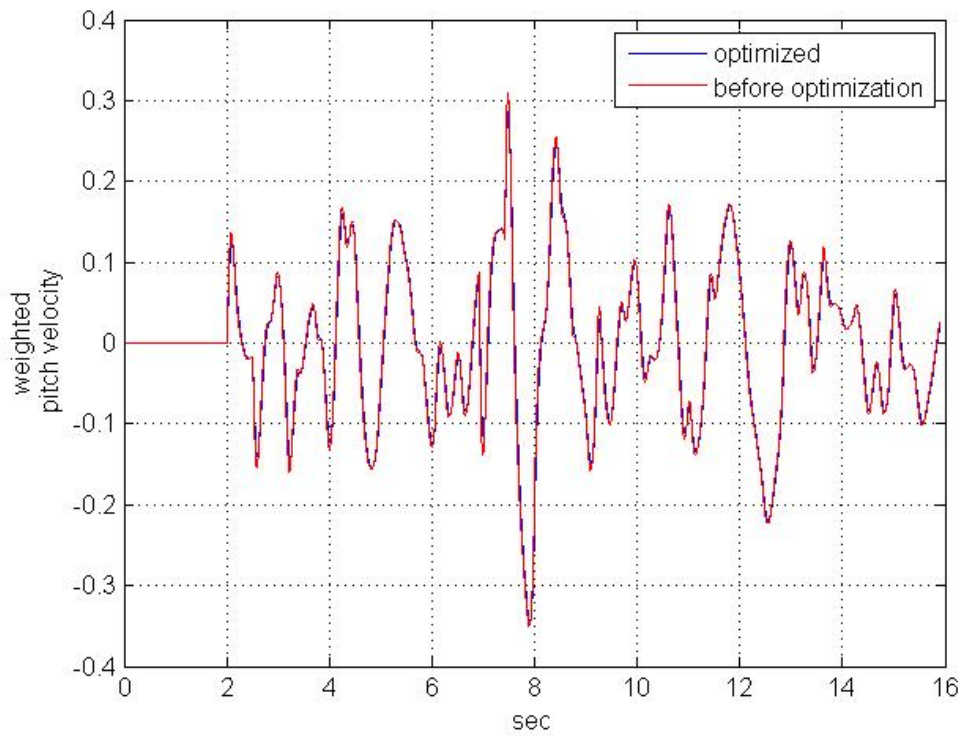


Figure 4.9 optimized weighted pitch velocity $\dot{\beta}$ for road profile one

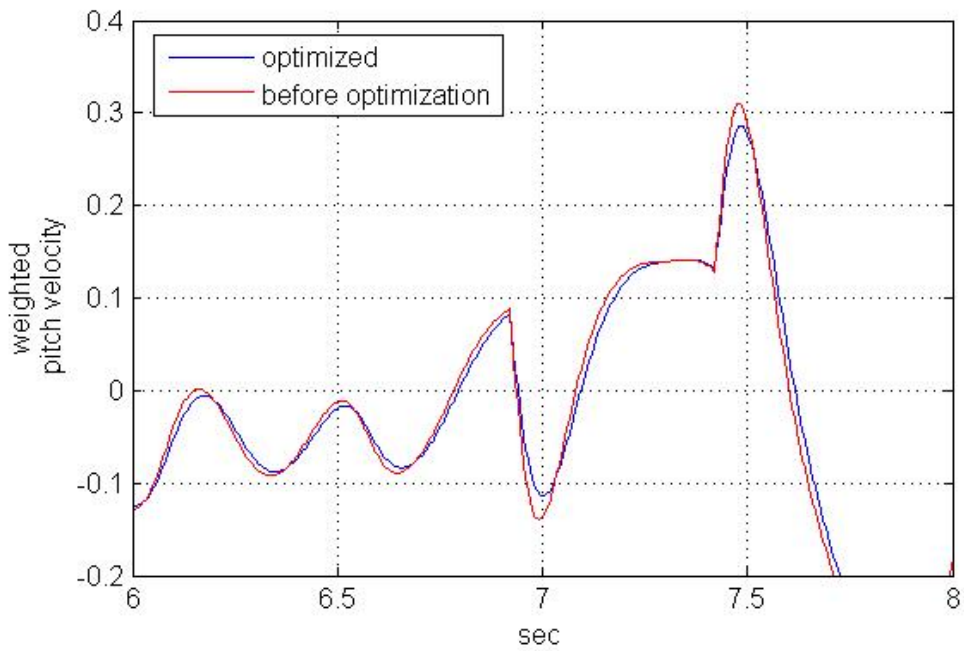


Figure 4.10 optimized weighted roll velocity $\dot{\beta}$ for road profile one
between 6 and 8 sec

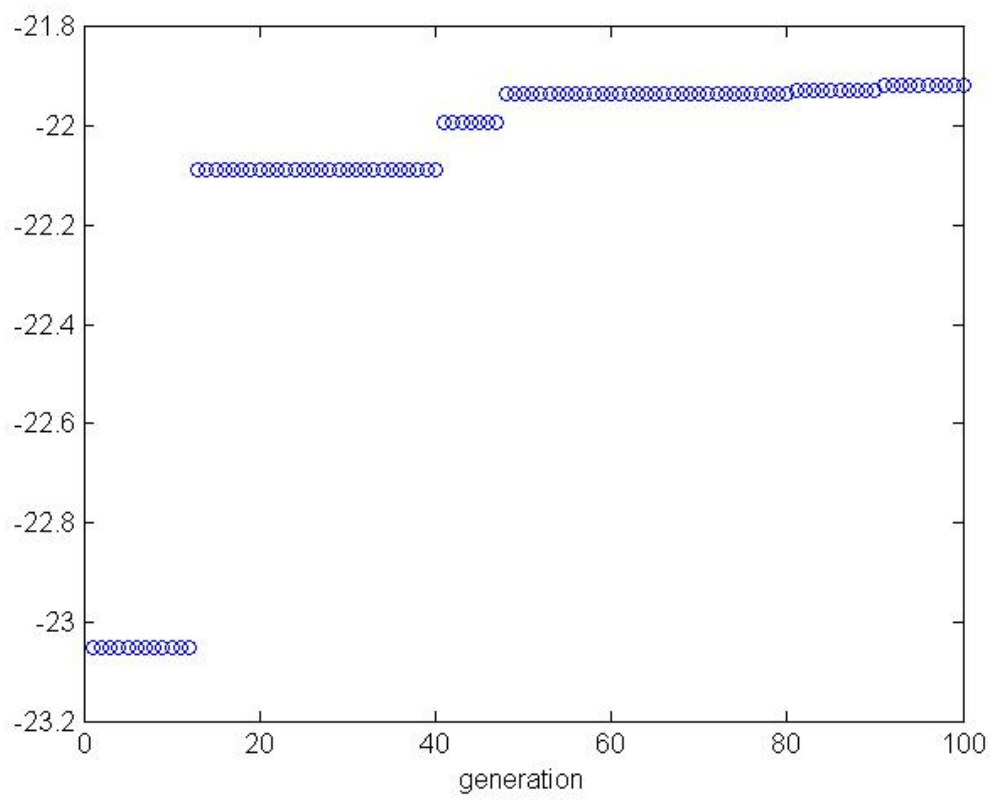


Figure 4.11 fitness of optimization for road profile one

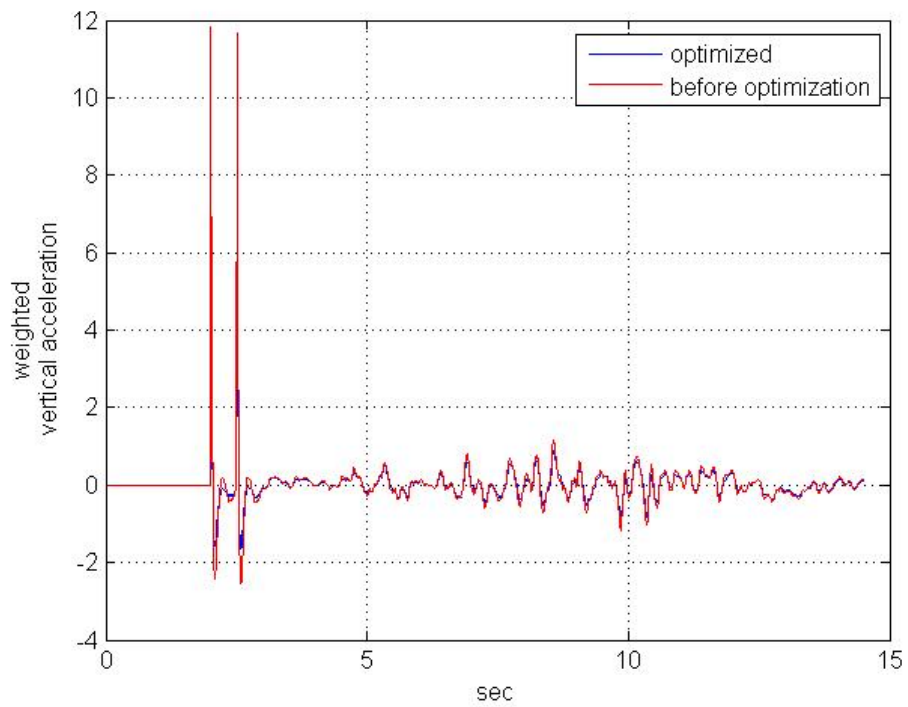


Figure 4.12 optimized weighted vertical acceleration \ddot{z} for road profile

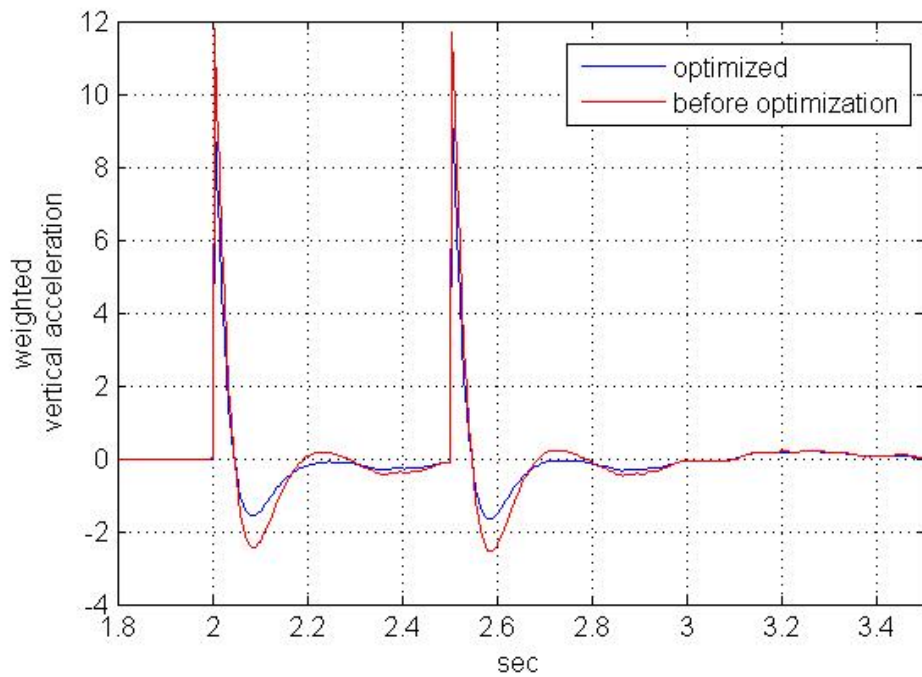


Figure 4.13 optimized weighted vertical acceleration \ddot{z} for road profile

two between 1.8 and 3.5 sec

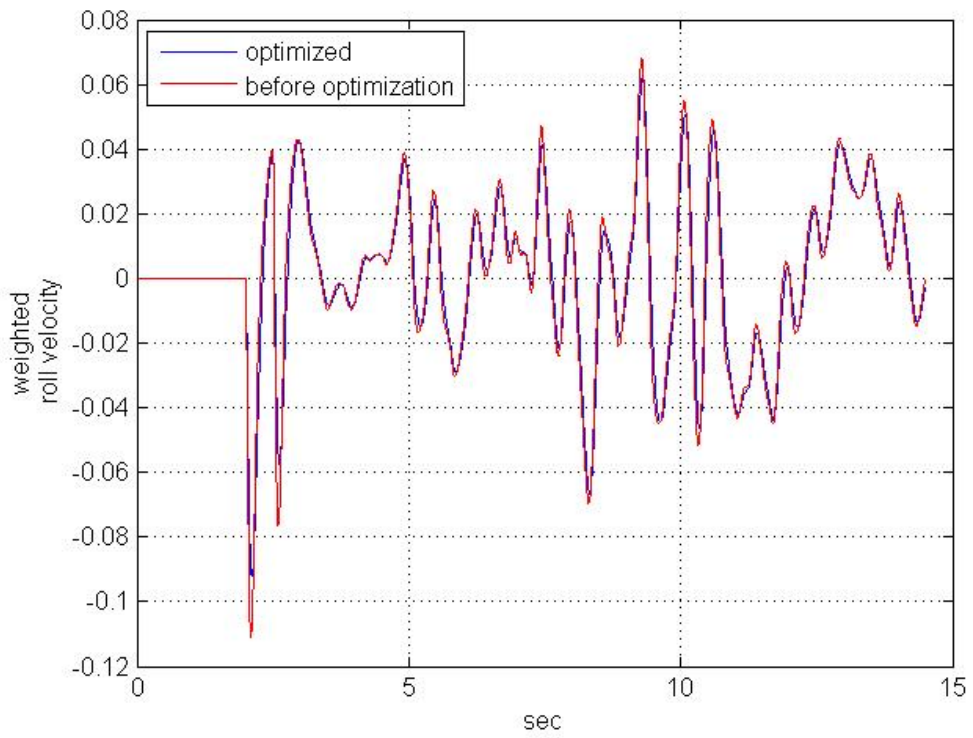


Figure 4.14 optimized weighted roll velocity $\dot{\alpha}$ for road profile two

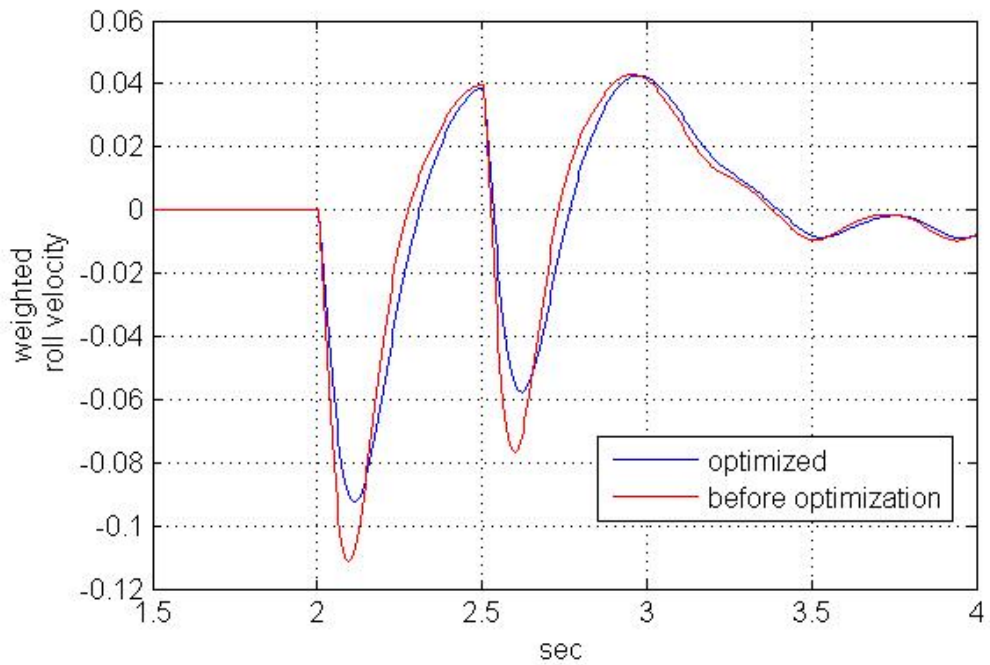


Figure 4.15 optimized weighted roll velocity $\dot{\alpha}$ for road profile two between 1.5 and 4 sec

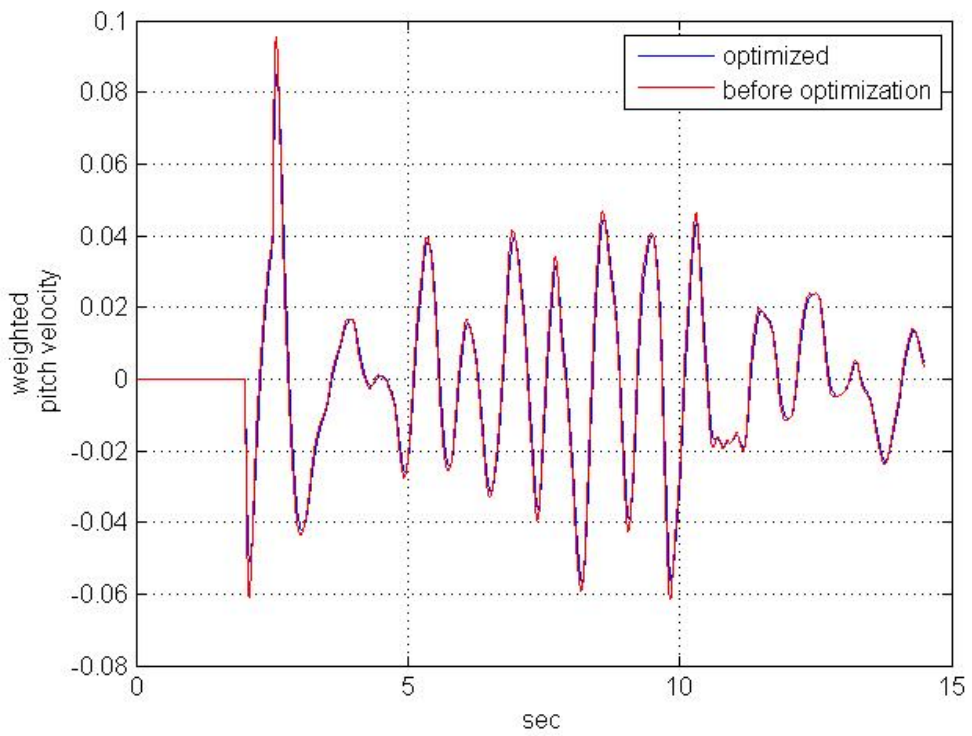


Figure 4.16 optimized weighted pitch velocity $\dot{\beta}$ for road profile two

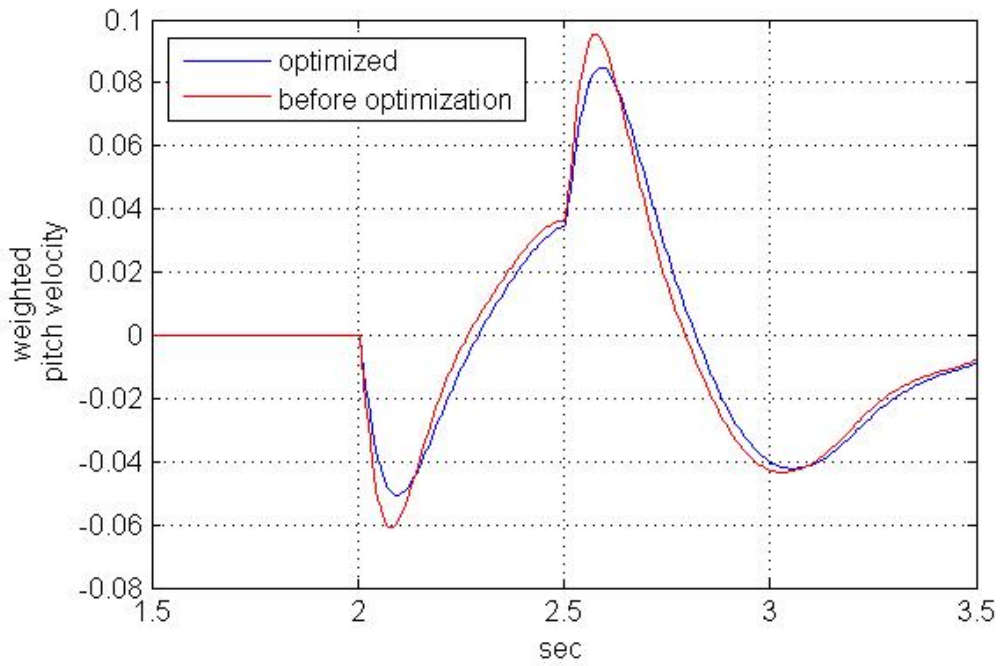


Figure 4.17 optimized weighted roll velocity $\dot{\beta}$ for road profile two
between 1.5 and 3.5 sec

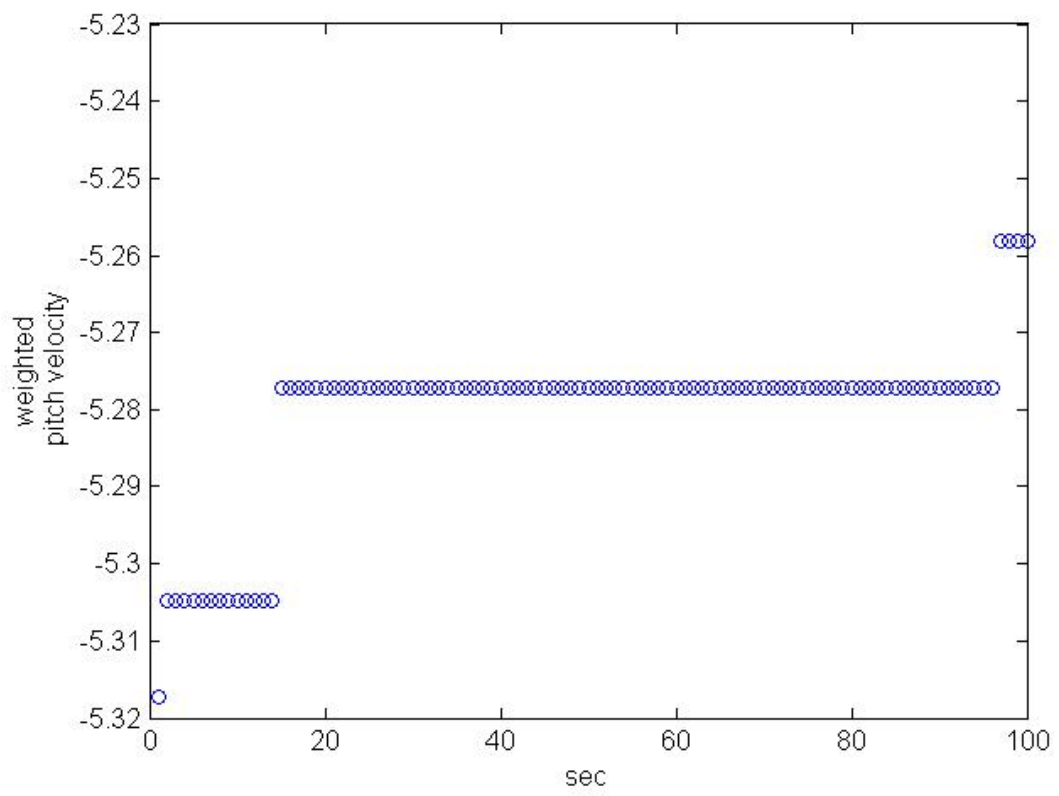


Figure 4.18 fitness of optimization for road profile two

Tables

Length	1.74 m
Width	1.06 m
Height	1.05 m
Dry weight	163.44 kg

Table 4.1 specification of Honda TRX250EX Sport ATV

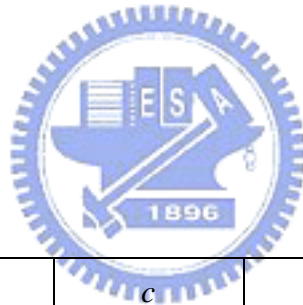


Generation number	Population size	Mutate rate
100	40	0.08

Table 4.2 settings of genetic algorithm

	k	c	VDV_z	J_α	J_β
Honda Trx250EX	22000	1200	16.8403	0.5442	0.3838
optimized	14480.6587	1002.6731	13.6141	0.5341	0.3765

Table 4.3 optimization results of road profile one



	k	c	VDV_z	J_α	J_β
Honda Trx250EX	22000	1200	4.28	0.0976	0.0878
optimized	12503.0626	1009.9273	3.4457	0.0921	0.0841

Table 4.4 optimization results of road profile two